

# A Virtual Screen Discovers Novel, Fragment-Sized Inhibitors of *Mycobacterium tuberculosis* InhA

Alexander L. Perryman,<sup>\*,†,‡,∇,○</sup> Weixuan Yu,<sup>§,○</sup> Xin Wang,<sup>||</sup> Sean Ekins,<sup>⊥,#</sup> Stefano Forli,<sup>†</sup> Shao-Gang Li,<sup>‡</sup> Joel S. Freundlich,<sup>‡,||</sup> Peter J. Tonge,<sup>§</sup> and Arthur J. Olson<sup>†</sup>

<sup>†</sup>Department of Integrative Structural and Computational Biology, The Scripps Research Institute, La Jolla, California 92037, United States

<sup>‡</sup>Center for Emerging & Re-emerging Pathogens, Division of Infectious Diseases, Department of Medicine, Rutgers University-New Jersey Medical School, Newark, New Jersey 07103, United States

<sup>§</sup>Institute for Chemical Biology & Drug Discovery, Department of Chemistry, Stony Brook University, Stony Brook, New York 11794, United States

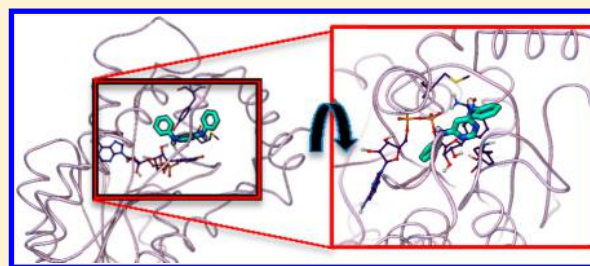
<sup>||</sup>Department of Pharmacology & Physiology, Rutgers University-New Jersey Medical School, Newark, New Jersey 07103, United States

<sup>⊥</sup>Collaborations in Chemistry, 5616 Hilltop Needmore Road, Fuquay-Varina, North Carolina 27526, United States

<sup>#</sup>Collaborative Drug Discovery, 1633 Bayshore Highway, Suite 342, Burlingame, California 94010, United States

## Supporting Information

**ABSTRACT:** Isoniazid (INH) is usually administered to treat latent *Mycobacterium tuberculosis* (*Mtb*) infections and is used in combination therapy to treat active tuberculosis (TB). Unfortunately, resistance to this drug is hampering its clinical effectiveness. INH is a prodrug that must be activated by *Mtb* catalase-peroxidase (KatG) before it can inhibit InhA (*Mtb* enoyl-acyl-carrier-protein reductase). Isoniazid-resistant cases of TB found in clinical settings usually involve mutations in or deletion of *katG*, which abrogate INH activation. Compounds that inhibit InhA without requiring prior activation by KatG would not be affected by this resistance mechanism and hence would display continued potency against these drug-resistant isolates of *Mtb*. Virtual screening experiments versus InhA in the GO Fight Against Malaria (GO FAM) project were designed to discover new scaffolds that display base-stacking interactions with the NAD cofactor. GO FAM experiments included targets from other pathogens, including *Mtb*, when they had structural similarity to a malaria target. Eight of the 16 soluble compounds identified by docking against InhA plus visual inspection were modest inhibitors and did not require prior activation by KatG. The best two inhibitors discovered are both fragment-sized compounds and displayed  $K_i$  values of 54 and 59  $\mu\text{M}$ , respectively. Importantly, the novel inhibitors discovered have low structural similarity to known InhA inhibitors and thus help expand the number of chemotypes on which future medicinal chemistry efforts can be focused. These new fragment hits could eventually help advance the fight against INH-resistant *Mtb* strains, which pose a significant global health threat.



## ■ INTRODUCTION

Tuberculosis (TB), caused by *Mycobacterium tuberculosis* (*Mtb*), kills 1.3 million people each year.<sup>1</sup> According to the World Health Organization (WHO), *Mtb* infects approximately 2 billion people.<sup>1</sup> Since a third of the global population has a latent *Mtb* infection, this creates an immense reservoir of disease due to the potential for reactivation.<sup>1</sup> There are 8.3 to 9 million new cases of TB annually, and half a million children get TB each year.<sup>1</sup> *Mtb* kills more people in the world than any other bacteria. Of all infectious diseases, only HIV kills more people than *Mtb*, and TB is the leading cause of death for HIV/AIDS patients.<sup>1</sup>

Although effective TB drugs have existed for over 60 years and drug-resistant TB was not a major issue 20 years ago,<sup>2</sup> cases of multidrug-resistant TB (MDR-TB) and extensively drug-

resistant TB (XDR-TB) continue to increase throughout the world in both frequency and distribution.<sup>1–7</sup> MDR-TB cases have nearly doubled in just a few years.<sup>4</sup> The global treatment success rate for TB is now less than 50%.<sup>1</sup> Each year, half a million new MDR-TB cases occur (i.e., *Mtb* infections that are resistant to isoniazid and rifampicin). XDR strains additionally evade fluoroquinolones and at least one of the second-line injectable drugs (amikacin, capreomycin, or kanamycin).<sup>1</sup> With the emergence of totally drug-resistant TB (TDR-TB) in several countries, no effective treatment options exist for these patients.<sup>3,5–8</sup>

Received: November 7, 2014

Published: January 30, 2015

**Novel InhA Inhibitors Effective against Isoniazid-Resistant Mutants Would Be Critical for Treating MDR- and XDR-TB.** InhA, an *Mtb* enoyl acyl-carrier protein reductase, is the primary target of the front-line drug isoniazid (INH).<sup>9,10</sup> While it is one of the two most important antitubercular drugs and the only drug used for TB prophylaxis, INH suffers from resistance that continues to increase.<sup>1,9,11,12</sup> WHO data indicate that up to 28% of all TB cases are INH-resistant, and in previously treated TB patients, up to 60% exhibit resistance, making it extremely difficult, time-consuming, and expensive to treat them (if they can be treated at all).<sup>1,2,13</sup>

INH must be activated by *Mtb* catalase-peroxidase (KatG).<sup>14–16</sup> Most clinically relevant INH-resistant *Mtb* strains involve mutations in or deletions of *katG*, which abrogate activation of the INH prodrug.<sup>17,18</sup> In some areas, 70% of MDR-TB strains have mutations in *katG*, as do 100% of sequenced XDR-TB strains.<sup>19,20</sup> Although *katG* mutations are generally responsible for high-level resistance to INH in clinical isolates, those mutations can be enhanced by additional mutations in the promoter region of *inhA*, which cause low-level INH resistance by increasing the amount of InhA produced<sup>21,22</sup> and are found in up to 28% of INH-resistant clinical isolates (depending on the location of the study).<sup>21–31</sup> KatG activates INH to enable the formation of a covalent adduct with NAD<sup>+</sup> or NADH.<sup>14</sup> As has been previously demonstrated, novel InhA inhibitors that do not require prior activation by KatG are not vulnerable to this key mechanism of INH resistance.<sup>11,17</sup>

Our virtual screen in this study was motivated by the clear need for a novel InhA-targeting drug that is effective against MDR- and XDR-TB strains. A next-generation InhA inhibitor that specifically lacks significant cross-resistance with INH by not requiring KatG activation would be a valuable addition to the antitubercular armamentarium and help stem the tide of TB drug resistance. Guiding our inhibitor discovery and design efforts are numerous X-ray crystal structures of InhA bound to cofactor, substrate mimic, or various inhibitors.<sup>10,11,32–44</sup> The pursuit of InhA inhibitors lacking the requirement for activation by KatG has transpired through both structure-based and screening approaches.<sup>12,45–48</sup> Notably, the Tonge group<sup>17,45,46,48</sup> and Freundlich et al.<sup>11</sup> have independently evolved potent triclosan-based inhibitors by leveraging X-ray crystal structures of InhA with bound diaryl ethers. However, a significant limitation of the triclosan scaffold has been the requirement for a phenol moiety, which suffers from rapid phase-II metabolism.<sup>49–51</sup> Our virtual screen focused on the NCI library to search for novel scaffolds that inhibit InhA without requiring prior activation by KatG and yet do not contain the problematic phenol group. Although many different factors affect in vivo pharmacokinetics and pharmacodynamics, especially when targeting a pathogen like *Mtb* that has an unusually thick and waxy cell wall and numerous efflux pumps and detoxification mechanisms, we sought to avoid the known liabilities that some current InhA inhibitors display.

High-throughput docking virtual screening (VS) studies have been used extensively in both academia and the pharmaceutical industry to discover inhibitors of selected drug targets (median hit rate of 13%<sup>52</sup>) and are complementary to experimental target-based high-throughput screening.<sup>53</sup> “Docking” flexible models of small molecules computationally probes the energetic landscape governing macromolecular recognition with a target protein to help guide the discovery and design

of novel inhibitors.<sup>54–61</sup> Docking flexible models of potential ligands against atomic-scale models of different protein drug targets may reproduce or predict (a) how tightly these compounds bind, (b) where they prefer to bind, and (c) what specific interactions they form at the binding site.

Many VS studies, including some against InhA, have involved computational studies in the absence of experimental validation of their predictions.<sup>62–68</sup> In contrast, some pioneering virtual screens against InhA have yielded predictions that were experimentally validated with enzyme inhibition assays<sup>69</sup> and/or whole-cell growth assays against *Mtb*,<sup>70,71</sup> *Mycobacterium vanbaalenii*,<sup>72</sup> and *Mycobacterium smegmatis*.<sup>73</sup> These previous, experimentally validated virtual screens against InhA helped establish the feasibility of computer-aided drug discovery against this system and laid the foundation for the research we present.

## ■ MATERIALS AND METHODS

### The Global Online Fight Against Malaria Project and Its Relevance to TB Research.

IBM's World Community Grid is a distributed network of over 2 million Internet-connected personal computers in over 80 countries, making it effectively one of the largest supercomputers available. It is entirely devoted to humanitarian research at academic and nonprofit institutions. The Global Online Fight Against Malaria (or “GO Fight Against Malaria”, GO FAM) was a project on World Community Grid that one of us (A.L.P.) designed and executed while at The Scripps Research Institute.<sup>74–76</sup> In under 2 years, GO FAM used over 27,385 CPU years to perform virtual screens of 5.6 million commercially available compounds against over 200 structures of targets from 22 classes of validated and potential drug targets for the treatment of malaria and other diseases. Using AutoDock Vina,<sup>61</sup> GO FAM generated a total of 1.16 billion docking results. These docking studies would have taken over a hundred years to complete using typical academic computing resources. The compound libraries screened were NCI, Enamine, Asinex, ChemBridge, and Vitas-M Laboratories, with 3D models obtained from the ZINC server.<sup>77</sup> *To the best of our knowledge, GO FAM is the first project to perform over a billion docking jobs, and it has produced the largest VS data sets against malaria and Mtb.*

If a malaria target had structural similarity with valid or potential drug targets from other pathogens whose crystal structures were available, the compounds were also docked against those cognate proteins, including *Mtb*, *Escherichia coli*, *Staphylococcus aureus*, *Yersinia pestis*, and *Brugia malayi*. The *Mtb* subset of GO FAM involved InhA, dihydrofolate reductase (DHFR), oxo-acyl ACP reductase (OAR or FabG), and cyclophilin A.

On GO FAM we docked a much larger number of compounds against InhA than in all previous virtual screens against it combined.<sup>64–73</sup> The results presented here encompass only 5.6% of the compounds screened on GO FAM against InhA—we began with the NCI library, because NCI compounds are available to researchers for free through the NCI's Developmental Therapeutics Program (DTP).

**Screening the NCI Library of Compounds against InhA on GO FAM.** The 316,000 pdbqt files generated for the NCI library (and for the other libraries that represent the 5.6 million compounds docked in the GO FAM experiments) are available at: <http://zinc.docking.org/pdbqt>. AutoDock Vina 1.1.2 (or “AD Vina”),<sup>61</sup> which was grid-enabled for World Community Grid by IBM staff, was used to dock each

compound in the library against the crystallographic conformation of InhA from 2X23.pdb.<sup>39</sup> In positive-control redocking experiments, the cocrystallized inhibitor PT70 docked to the target model of 2X23 with a root-mean-square deviation (RMSD) of 0.49 Å. Additional (successful) positive-control redocking and cross-docking experiments that utilized AD Vina against other crystal structures of InhA bound to different ligands have been published recently elsewhere.<sup>78</sup> This 2X23 structure of InhA was selected for the present study, because it is a complex with PT70, a slow, tight-binding inhibitor of InhA with an inhibition constant ( $K_i$ ) of 7.8 nM and a residence time of 24 min. Displaying a long residence time with a pathogenic target imparts favorable properties *in vivo*.<sup>79–81</sup> Using the PT70-induced conformation may enable us to identify and develop novel inhibitors that display long residence times with InhA. The ambitiousness of this goal necessitated the resources of GO FAM to screen 5.6 million compounds against this and other crystal structures of InhA. Hydrogen atoms were added to the target model using the MolProbity server.<sup>82</sup> Crystallographic waters and counterions were deleted from the pdb file. AutoDockTools 4.2<sup>83</sup> was then used to generate the pdbqt file. A 30 Å × 30 Å × 30 Å grid box centered between the N9 atom of adenine and C1 of the adjacent ribose in the NAD cofactor defined the region that the docked compounds explored. This location and large size were selected to enable the same grid box to be used for all of the different InhA and PfENR targets that were part of these GO FAM experiments. The “exhaustiveness” setting in AD Vina was increased to 20 (from the default of 8) because of the large grid box used.

**Target-Specific Energetic and Interaction Filtering of VS Results.** We characterized the predicted binding mode of each compound in the NCI library by the number and types of energetically favorable interactions with the InhA active site and the estimated free energy of binding using a software-automated workflow (python and tc-shell scripts) and established protocols.<sup>84–86</sup> The results were filtered to harvest compounds that displayed critical interactions (based on analyses of the features displayed by nanomolar inhibitors of InhA in existing crystal structures).<sup>11,35,39,41</sup> These filters selected compounds for which the top-scoring binding mode/compound displayed base-stacking interactions between the candidate compound and the NAD<sup>+</sup>/NADH cofactor and at least two predicted hydrogen bonds to the active site. The selected compounds also had to display an estimated free energy of binding (FEB) less than or equal to −8.0 kcal/mol according to the AD Vina scoring function. This set of docking filters harvested 91 compounds, whose binding modes were then visually inspected (see Figure 1).

Visual inspection is a subjective process, but experience in macromolecular recognition and knowledge of the strengths and weaknesses of different modeling approaches used to view, measure, and judge/prioritize the docked results can be helpful. The use of human knowledge (“in cerebro” quality control) to prioritize computer-aided (“in silico”) predictions has been a successful strategy in previous blind docking challenges, such as SAMPL2 and SAMPL4.<sup>86–88</sup> Our visual inspection process incorporated multiple criteria in an attempt to decrease the number of false positives that often result from virtual screens. Unfavorable aspects of a docking result included compounds that (a) have docked modes displaying distorted geometries (i.e., peptide bonds in the ligand models were allowed to freely rotate during docking, since the target was rigid, but docked

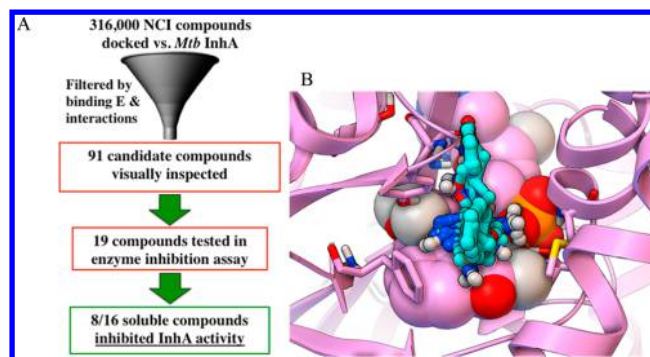


**Figure 1.** Workflow used to discover novel InhA inhibitors in the virtual screen with the NCI library on GO FAM. (A) The workflow used energy- and interaction-based filters (i.e., requiring compounds to display an estimated free energy of binding less than or equal to −8.0 kcal/mol, to base-stack with the NAD cofactor, and to form at least two hydrogen bonds with the active site) to filter the VS results and harvest NCI compounds for visual inspection. Candidates that passed visual inspection were then ordered and tested in InhA inhibition assays. Eight of the 16 soluble compounds inhibited InhA activity by 27–71% at 100  $\mu$ M. (B) The predicted binding modes for all eight novel InhA inhibitors are displayed in ball-and-stick mode with cyan carbons, while the InhA target is shown in magenta. The NAD cofactor is rendered as CPK, and the key residues Gly96, Ser123, Phe149, Tyr158, Thr196, and Met199 are shown as thin sticks.

modes displaying peptide bonds that were 30–90° from cis or trans were rejected); (b) have one or more large hydrophobic groups (e.g., phenyl or *tert*-butyl) exposed to solvent; or (c) display more than three unfavorable electrostatic repulsion interactions with polar or charged groups in the target. Favorable aspects of a docked pose included compounds where (d) a majority of their heteroatoms are involved in favorable electrostatic interactions or hydrogen bonds (as discussed in our recent article),<sup>78</sup> since heteroatoms will likely need to be added during the optimization process without violating Lipinski’s rules;<sup>89</sup> (e) the hydrophobic groups display van der Waals interactions with nonpolar regions of the target (as measured by the AD Vina scoring function,<sup>61</sup> characterized using distance-dependent and atom-pair-specific criteria implemented in the Fox software<sup>84</sup>); and (f) aromatic rings displayed  $\pi$ – $\pi$  (base-stacking or T-stacking)<sup>90–92</sup> or  $\pi$ –cation interactions with the target,<sup>91–93</sup> as characterized by the Fox software.<sup>84</sup> The AD Vina scoring function uses ambiguous atom types (i.e., hydrogen-bond donors are treated as donor and/or acceptor) and a spherical hydrogen-bonding potential (instead of an angle-dependent potential).<sup>61</sup> Consequently, to verify the number of hydrogen bonds that the docking filters detected, the donor–acceptor distances and donor–hydrogen–acceptor angles (which should be between 120 and 180°) for predicted hydrogen bonds were all measured manually in PMV.<sup>83</sup> Because rotatable polar hydrogen atoms in the ligands are placed in arbitrary torsion angles by AD Vina<sup>61</sup> and the model of the target was rigid, structural intuition was also employed when deciding which hydrogen bonds the docked mode displayed. Special emphasis was placed on candidates that (g) displayed hydrogen bonds with invariant residues and backbone atoms, since previous studies with MDR HIV protease and MDR *Plasmodium falciparum* DHFR have shown that displaying these features renders the evolution of drug resistance less likely.<sup>94–110</sup>

**InhA Inhibition and Kinetics Experiments.** An InhA inhibition assay was performed on the selected candidate



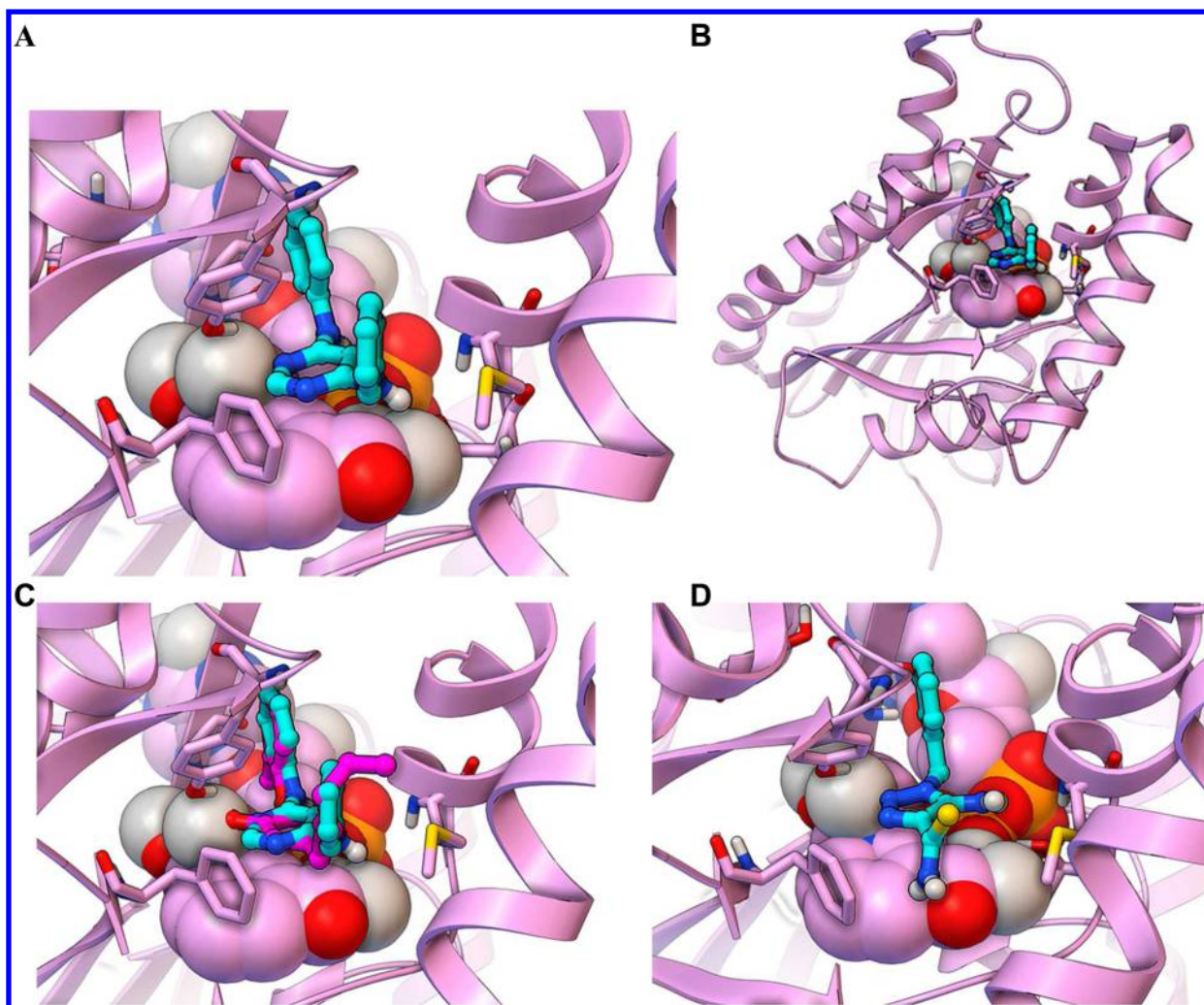


**Figure 2.** Predicted binding modes of the two most potent new InhA inhibitors discovered in GO FAM experiment 5. The docked modes produced by AutoDock Vina are displayed in ball-and-stick mode with cyan carbon atoms, and the InhA target (2X23.pdb) is displayed as magenta ribbons. The NAD cofactor is displayed in CPK, and the key residues Gly96, Ser123, Phe149, Tyr158, Thr196, and Met199 are shown as thin sticks. (A) Close-up view and (B) full view of the predicted binding mode of the top fragment hit, NCI 99389 ( $K_i^{\text{app}} = 54.1 \pm 5.4 \mu\text{M}$ ). (C) Comparison of the docked mode of NCI 99389 to the experimentally determined binding mode of PT70, the inhibitor crystallized with InhA in 2X23.pdb, which is displayed in ball-and-stick mode with magenta carbons. (D) Predicted binding mode of the second-most-potent fragment hit, NCI 111591 ( $K_i^{\text{app}} = 59.2 \pm 8.7 \mu\text{M}$ ).

compounds. Briefly, the candidate inhibitor was assayed at 100  $\mu\text{M}$  in a reaction buffer (30 mM PIPES, 150 mM NaCl, 1 mM EDTA, pH 6.8) containing 30  $\mu\text{M}$  *trans*-2-dodecenoyl coenzyme A (DD CoA), 250  $\mu\text{M}$  NADH, and 100 nM InhA. The enzymatic activity at 100  $\mu\text{M}$  inhibitor concentration was quantified, and the three compounds that displayed the largest inhibition of enzyme activity were selected for further median inhibitory concentration ( $\text{IC}_{50}$ ) measurements. In general,  $\text{IC}_{50}$  values were determined by varying the concentration of the inhibitor in the aforementioned reaction mixture. The data were analyzed using eq 1:

$$y = \frac{100\%}{1 + \frac{[I]}{\text{IC}_{50}}} \quad (1)$$

where  $[I]$  is the inhibitor concentration and  $y$  is the percent activity.

To provide mechanistic insight, the top two compounds were chosen for subsequent measurements of  $K_i$ . The third-best inhibitor displayed solubility problems at higher concentrations.

The  $K_i$  value was calculated by determining the  $k_{\text{cat}}$  and  $K_M$  (DD CoA) values at several fixed inhibitor concentrations using the assay conditions described above. The data were analyzed using the standard equations for competitive and non-competitive inhibition (eqs 2 and 3):

$$v_0 = \frac{v_{\text{max}}[S]}{K_M \left( 1 + \frac{[I]}{K_i} \right) + [S]} \quad (2)$$

$$v_0 = \frac{v_{\text{max}}[S]}{K_M \left( 1 + \frac{[I]}{K_i} \right) + [S] \left( 1 + \frac{[I]}{K'_i} \right)} \quad (3)$$

**Comparison of the New InhA Inhibitors to Known InhA Inhibitors.** To assess the chemical property space of the eight InhA inhibitors found, principal component analysis (PCA) was performed on the combination of the 157 known InhA inhibitors in TB Mobile 2 and the eight inhibitors discovered.<sup>111,112</sup> The sdf of the TB Mobile data set was used for the PCA, which was calculated using Discovery Studio

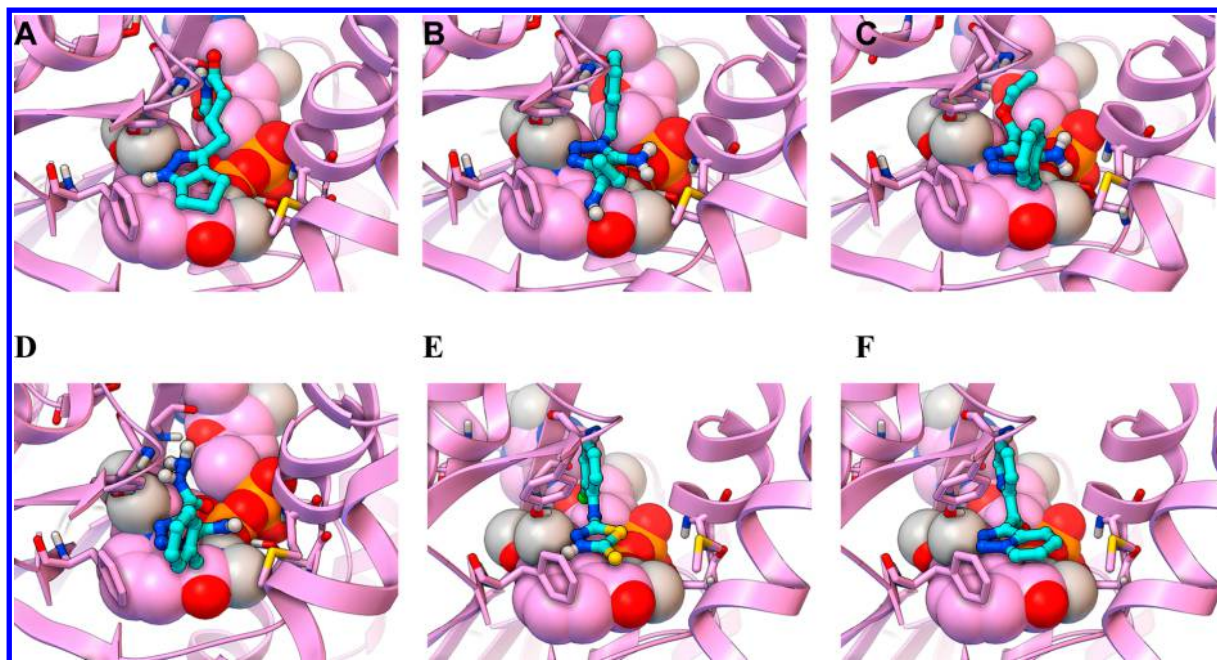


**Figure 3.** Predicted binding modes of the least potent new InhA inhibitors discovered in GO FAM experiment 5: (A) NSC 112144 ( $K_i^{\text{app}} = 205.6 \pm 46 \mu\text{M}$ ); (B) NSC 111589; (C) NSC 111590; (D) NSC 111588; (E) NSC 135809; (F) NSC 196166. The docked modes produced by AutoDock Vina are displayed in ball-and-stick mode with cyan carbon atoms. The InhA target (2X23.pdb) is displayed as magenta ribbons, with the NAD cofactor in CPK. The key residues Gly96, Ser123, Phe149, Tyr158, Thr196, and Met199 are shown as thin sticks.

3.5<sup>113</sup> and used eight interpretable descriptors (AlogP, molecular weight, number of rotatable bonds, number of rings, number of aromatic rings, number of hydrogen-bond acceptors, number of hydrogen-bond donors, and molecular fractional polar surface area).

The pairwise Tanimoto similarity<sup>114</sup> was calculated for each of the new InhA inhibitors discovered in the NCI library versus each of the 154 known InhA inhibitors from TB Mobile.<sup>111</sup> This again used the TB Mobile data set sdf, for which MDL descriptors were calculated, followed by Tanimoto similarity using the “find similar molecules by fingerprints” protocol in Discovery Studio 3.5.<sup>113</sup> This then enabled us to calculate the minimum, maximum, and average similarities as measures of proximity to known InhA inhibitors.

The pairwise Tanimoto similarity<sup>114</sup> was also calculated for each of the eight new InhA inhibitors versus each of the seven other compounds in order to determine the number of distinct scaffolds, according to a cutoff of  $>0.7$ <sup>115</sup> (see Table S1 in the Supporting Information).

#### Minimum Inhibitory Concentration Assay versus *Mtb*.

For these whole-cell in vitro studies, new batches of NCI 99389 and 111591 were obtained from the NCI. LC–MS data confirmed that each sample had the expected molecular weight and was  $>97\%$  pure by HPLC at 250 nm (see Figures S1–S2 and S4–S5 in the Supporting Information). <sup>1</sup>H NMR spectroscopy (600 MHz) using DMSO-*d*<sub>6</sub> and acetone-*d*<sub>6</sub> as NMR solvents for 99389 for 111591, respectively, confirmed that each sample had the expected structure (see Figures S3 and S6 in the Supporting Information). Minimum inhibitory concentration (MIC<sub>90</sub>) values of the compounds were determined following the microplate-based Alamar Blue assay (MABA) method as previously described.<sup>116</sup> Stock solution (50 mM compound in DMSO) was dissolved in sterile Middlebrook 7H9-OADC broth, making a 1 mM pretest solution, and 100  $\mu\text{L}$  aliquots of pretest solution were added

into wells in column 1 of a sterile polystyrene 96-well round-bottom plate (CLS3795, Corning, NY). Wells in columns 2–12 received 50  $\mu\text{L}$  of sterile 7H9-OADC broth. Serial 2-fold dilutions of compounds were performed, and column 12 was set as a drug-free (inoculum-only) control. The final concentrations of compounds were as follows: for INH, 0.012–25  $\mu\text{g}/\text{mL}$ ; for NCI 99389 and 111591, 0.50–500  $\mu\text{M}$ . *M. tuberculosis* wild-type strain H37Rv and the *inhA* overexpression strain mc<sup>2</sup>4914 (see ref 10) were diluted 1:1000 in 7H9+OADC medium at mid-logarithmic stage of growth (optical density at 595 nm = 0.4), and 50  $\mu\text{L}$  of diluted bacteria suspension was inoculated into each well. The plates were sealed with Parafilm and incubated at 37 °C for 7 days. Next, 20  $\mu\text{L}$  of Alamar Blue reagent (Invitrogen, Frederick, MD) freshly mixed with 12.5  $\mu\text{L}$  of 20% Tween 80 was added to each well, followed by incubation for 24 h at 37 °C. The absorbance was read at 570 nm, with a reference wavelength of 600 nm, using a microplate reader (ELX808, Biotek Instruments). The MIC<sub>90</sub> end point was defined as the lowest concentration of the test agent that produced at least a 90% reduction in absorbance compared with that of the drug-free control.

**Cellular Toxicity Assay.** The cytotoxicities of 99389 and 111591 were determined by the 3-(4,5-dimethylthiazol-2-yl)-2,5-diphenyltetrazolium bromide (MTT) cytotoxicity assay with the Vybrant MTT Cell Proliferation Assay Kit (Molecular Probes).<sup>13</sup> Vero cells (African green monkey kidney epithelial cells; ATCC) were plated in a sterilized 96-well plate (Costar 3595, Corning, NY) at  $2 \times 10^5$  cells/well with a volume of 50  $\mu\text{L}$  and incubated for 3 h in a 37 °C incubator. 99389 and 111591 were dissolved in DMSO at a final concentration of 10 mg/mL. In a separate 96-well plate, 2-fold serial dilutions were performed with Dulbecco’s modified Eagle’s medium (Gibco) supplemented with 10% fetal bovine serum, and 50  $\mu\text{L}$  aliquots of diluted compounds were added to appropriate test plate wells to generate final concentrations ranging from 0.78 to 100



$\mu\text{g/mL}$ . Column 12 was utilized as a drug-free control. After treatment for 48 h, 10  $\mu\text{L}$  of 12 mM MTT stock solution was added to each well, and the wells were incubated at 37  $^{\circ}\text{C}$  for 4 h. Subsequently, 100  $\mu\text{L}$  of 0.1 g/mL SDS-HCl solution was added into each well to halt the reaction, followed by incubation for 4 h at 37  $^{\circ}\text{C}$ . The absorbance at 570 nm was read with a VersaMax ELISA microplate reader (Molecular Devices). The median cytotoxic concentration ( $\text{CC}_{50}$ ) was extrapolated by plotting the absorbance at 570 nm versus the concentration of the untreated Vero cells control.

## RESULTS AND DISCUSSION

This pilot study of a small subset (i.e., 5.6%) of the GO FAM results versus InhA led to the discovery of several novel inhibitors (see Figures 2–4). Nineteen compounds were

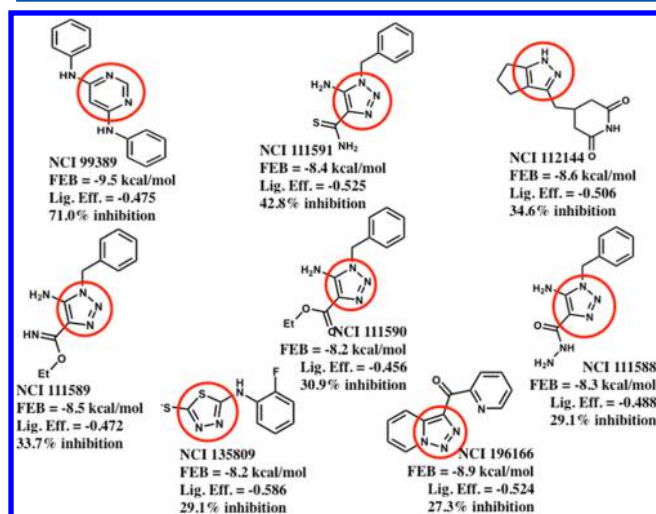


**Figure 4.** Summary of the 2D structures, docking scores, and InhA inhibitory activities of the eight new inhibitors discovered. The most potent new InhA inhibitor discovered is shown in the top-left corner, while the least potent new inhibitor is displayed in the bottom-right corner. These eight new inhibitors correspond to five novel scaffolds versus InhA (i.e., NCI 111588–111591 represent analogs of one scaffold, according to a Tanimoto cutoff of 0.7; see Table S1 in the Supporting Information). FEB signifies the estimated free energy of binding from AutoDock Vina's scoring function, in kcal/mol. Lig. Eff. is the calculated ligand efficiency from AutoDock Vina, in kcal/mol per heavy atom. The % inhibition of InhA activity was obtained when each compound was present at 100  $\mu\text{M}$ . The region of each compound that was predicted to base-stack with the NAD cofactor is highlighted with a red circle.

ordered, but three of them were insoluble at 100  $\mu\text{M}$  in DMSO and could not be assayed (see Table 1). Eight of the 16 soluble candidates were modest inhibitors of InhA (i.e., showing 27–71% inhibition at 100  $\mu\text{M}$ ). Under the same assay conditions and protocol (i.e., without preincubation of the compound and InhA), the very potent positive-control compound PT70 displayed 75% inhibition at 100 nM (i.e., the well-optimized lead compound PT70 was >1000 times more potent than our best new inhibitor). If scaffolds are defined as small-molecule chemotypes that possess less than 70% similarity according to Tanimoto values,<sup>115</sup> these eight inhibitors represent five novel scaffolds against InhA (see Figure 4 and Table S1 in the Supporting Information). As required by the docking filters, all eight compounds are predicted to base-stack with the NAD cofactor (see Figures 2

and 3) instead of forming a covalent adduct with it. As demonstrated by the InhA activity assays, they do not require prior activation by *Mtb* KatG. “Hits” were classified in a way that involved the potency for a particular size of compound. “Fragment hits” (novel inhibitors with molecular weight (MW) less than 300 Da)<sup>117</sup> tend to display potencies in the hundreds micromolar to low-millimolar range (according to  $K_i$  or  $K_d$ ).<sup>87,117–123</sup> Consequently, we defined fragment hits as novel inhibitors with MW < 300 g/mol that displayed  $K_i$  values of <100  $\mu\text{M}$ . Two of our inhibitors are “fragment hits”: they are structurally distinct from known InhA inhibitors (see Figures 2 and 5 and Table 2), and they displayed  $K_i$  values of  $54.1 \pm 5.4$  and  $59.2 \pm 8.7$   $\mu\text{M}$ , respectively (see Figure 6). Thus, on the basis of a stringent metric, two out of 16 compounds were novel fragment hits against InhA (i.e., a 12.5% hit rate), representing two promising new scaffolds.

The most promising new scaffold, NCI 99389, is a 4,6-diaminopyrimidine and was predicted to form the following quaternary interactions in the docking studies: base-stacking with the nicotinamide ring of the NAD cofactor (similar to the crystallographic binding mode of PT70);<sup>39</sup> T-stacking with the side chain of Phe149; hydrogen-bonding with the hydroxyl of Tyr158 (similar to PT70);<sup>39</sup> hydrogen-bonding with the 2'-hydroxyl of the ribose adjacent to the nicotinamide ring of NAD (similar to PT70);<sup>39</sup> hydrogen-bonding with the sulfur in the side chain of Met199; favorable electrostatic interactions with the hydroxyl of Tyr158; and favorable electrostatic interactions with the phosphate group proximal to the ribose of NAD (see Figure 2A). As a reference, in addition to the aforementioned hydrogen-bonding and base-stacking interactions that the crystallographic binding mode of PT70 displays, PT70 also contains a six-carbon alkyl tail that packs very well into a hydrophobic pocket of InhA. Despite the use of a large grid box in these docking calculations (i.e., allowing the ligands to sample a large volume of the protein), docking calculations suggested a clear preference for 99389 to bind in a fashion similar to the crystallographic binding mode of PT70 (see Figure 2C). Experimental structure verification will be necessary to firmly establish the actual binding mode. Since this compound is an unoptimized fragment hit and lacks the long alkyl tail that PT70 contains, it might not produce the same “closed” conformation that PT70 induces<sup>39,124</sup> (which might give 99389 a different binding mode than predicted by these docking calculations) and/or it might have to pay a larger enthalpic penalty to induce the ligand-bound conformation that InhA forms (which, when combined with the numerous hydrophobic contacts that it lacks, might also explain part of the >1000-fold difference in potency vs PT70). NCI 99389 displayed an  $\text{IC}_{50}$  of approximately 40  $\mu\text{M}$  against InhA (see Table 1). In subsequent kinetic experiments (see Figure 6 and Table 1), it displayed an apparent  $K_i$  ( $K_i^{\text{app}}$ ) of  $54.1 \pm 5.4$   $\mu\text{M}$  and demonstrated a competitive mechanism of inhibition with respect to substrate.

The second most promising new scaffold discovered, NCI 111591, is a 5-amino-1*H*-1,2,3-triazole and had a docked mode displaying the following quaternary interactions with InhA: base-stacking with the nicotinamide ring of the NAD cofactor; hydrogen-bonding with the hydroxyl of Tyr158; hydrogen-bonding with the 2'-hydroxyl of the ribose adjacent to the nicotinamide ring of NAD; hydrogen-bonding with the carbonyl oxygen of the nicotinamide ring; favorable electrostatic interactions with the sulfur in the side chain of Met199; favorable electrostatic interactions with the phosphate group

Table 1. Compound IDs, 2D Structures, and InhA Inhibition Data<sup>a</sup>

NCI ID	Structure	K <sub>i</sub> <sup>app</sup> (μM) & mechanism	InhA inhibition at 100 μM inhibitor
660846			2.7%
683622			9.2%
609097			10.3%
314884			10.3%
371850			Not soluble
11142			4.5%
75300			Inhibitor precipitated in buffer
75301			Inhibitor precipitated in buffer
<b>99389</b> (ZINC01654204)		<b>54.1 ± 5.4</b> <b>competitive</b>	<b>71.0%</b> (estimated IC <sub>50</sub> ~ 40 μM)
111588 (ZINC01350777)			29.1%
111589 (ZINC04994329)			33.7%
111590 (ZINC00129134)			30.9%
<b>111591</b> (ZINC01703321)		<b>59.2 ± 8.7</b> <b>noncompetitive</b>	<b>42.8%</b>
112144 (ZINC04878446)		205.6 ± 46 (precipitation observed at high concentrations)	34.6%
130836			9.1%
135809 (ZINC01722139)			29.1%
196166 (ZINC01734860)			27.3%
213837			10.9%
293934			9.1%

<sup>a</sup>Each compound was initially tested at a single concentration. Only the top inhibitors (highlighted in **bold font**) were subjected to additional experimental characterization. For the top eight new inhibitors, both the NCI ID and the ZINC ID are displayed.

proximal to the ribose of NAD; and favorable electrostatic interactions with the 2'-hydroxyl of the ribose adjacent to the nicotinamide ring of NAD (see Figure 2D). When present at 100 μM, NCI 11591 exhibited 42.8% inhibition of InhA activity. It displayed an apparent K<sub>i</sub> of 59.2 ± 8.7 μM. As shown in Figure 6, 111591 followed a noncompetitive mechanism of inhibition (i.e., it can bind when the substrate is “not on or on,” meaning it could potentially bind to the holo enzyme, to the InhA–substrate complex, and/or to the InhA–NAD<sup>+</sup>–product complex). To further confirm the inhibition mode, data were fit to both eq 2 and eq 3 for comparison. The K<sub>i</sub> values generated from the noncompetitive and competitive fits were 59.2 ± 8.7

and 54.0 ± 51.0 μM, respectively. The much greater error for the competitive fit unambiguously confirmed the inhibition mechanism as noncompetitive.

The predicted binding modes for the six less potent (and thus less promising) new InhA inhibitors discovered are presented in Figure 3. They were all predicted to base-stack with the nicotinamide ring of the NAD cofactor and to form a hydrogen bond with the hydroxyl of Tyr158. Five of the six inhibitors (i.e., all except NCI 111590) docked to form both a hydrogen bond and an additional favorable electrostatic interaction with the 2'-hydroxyl of the ribose adjacent to the nicotinamide ring of NAD, but the predicted pose of 111590

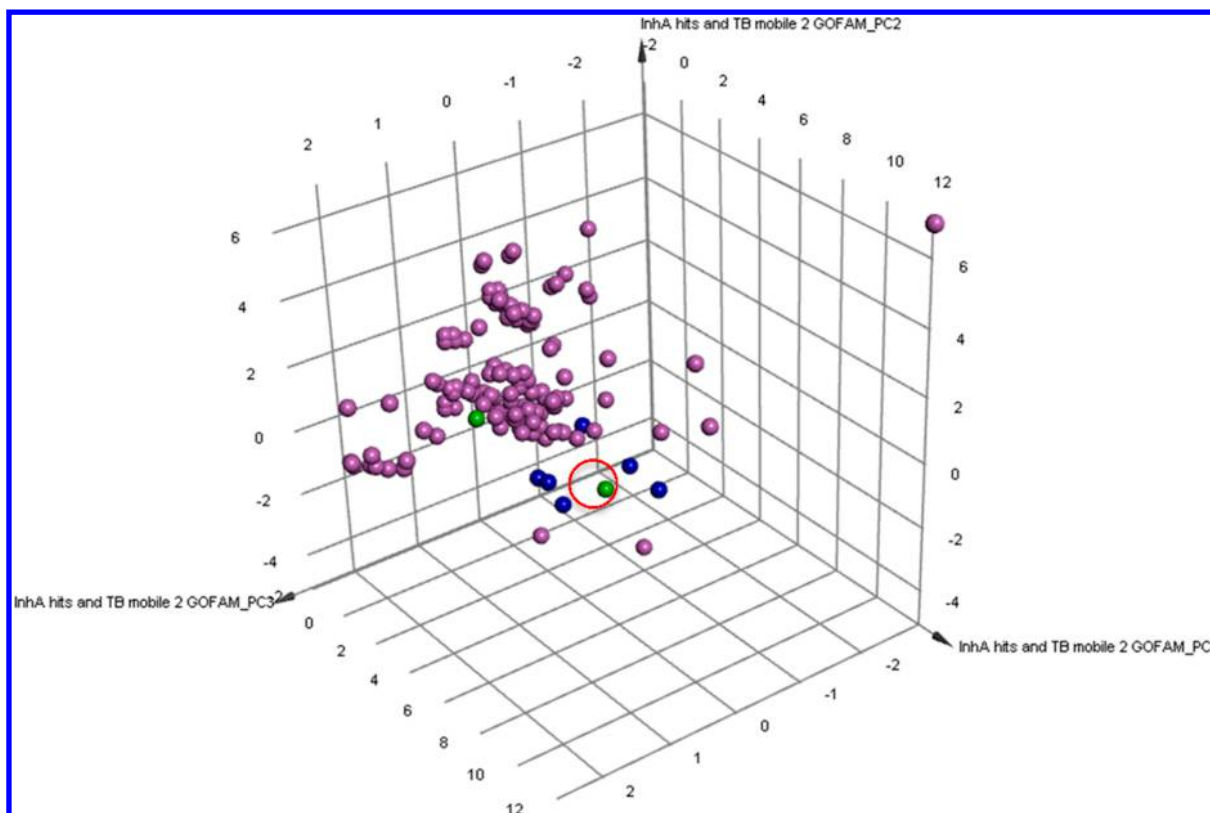


**Figure 5.** Comparison of the chemical space of the new InhA inhibitors to that of known InhA inhibitors. Principal component analysis (PCA) was performed on the combination of the 157 known InhA inhibitors in the TB Mobile 2 data set and the eight novel InhA inhibitors discovered. Three PCs explain 84.8% of the variance observed. The 157 InhA inhibitors in the TB Mobile 2 data set are displayed in magenta. The two most potent new InhA inhibitors discovered are depicted in green, and the other six novel InhA inhibitors identified are in blue. A red circle highlights the location of NCI 111591. The PCA indicates that the eight new InhA inhibitors have chemical properties similar to those of known InhA inhibitors but are generally not within the main clusters of these previously characterized InhA inhibitors.

**Table 2. Tanimoto Similarities of the Eight Novel Inhibitors to the 154 Known InhA Inhibitors in the TB Mobile Data Set**

compound IDs	similarities		
	average	maximum	minimum
NCI 99389 (ZINC01654204)	0.3087	0.4130	0.1458
NCI 111591 (ZINC01703321)	0.3681	0.4634	0.1311
NCI 112144 (ZINC04878446)	0.4503	0.5738	0.15
NCI 111589 (ZINC04994329)	0.4307	0.5732	0.1642
NCI 111590 (ZINC00129134)	0.4296	0.5522	0.1935
NCI 111588 (ZINC01350777)	0.4542	0.5897	0.1406
NCI 135809 (ZINC01722139)	0.2731	0.4366	0.1061
NCI 196166 (ZINC01734860)	0.3551	0.4833	0.1724

only formed a favorable electrostatic interaction with that hydroxyl. 112144 was also predicted to form a hydrogen bond with the carbonyl of Gly96, but it was predicted to display unfavorable electrostatic repulsions with both phosphate groups of the NAD cofactor. The amino nitrogen and ether oxygen atoms of 111589 were predicted to form favorable and unfavorable electrostatic interactions, respectively, with the sulfur in the side chain of Met199, and it displayed an internal hydrogen bond between that amino group and the ether oxygen. The conserved regions of the scaffolds in 111590 and 111588 had docked modes that superimposed, and they formed favorable electrostatic interactions with the sulfur in the side chain of Met199 and the hydroxyl of Ser123. If a slight

conformational change occurs in the side chain of Phe149, they could both T-stack with it. Docking of 135809 suggested that favorable electrostatic interactions could be formed with the phosphate group adjacent to the ribose of the NAD cofactor, but it formed unfavorable electrostatic repulsions with both the sulfur in the side chain of Met199 and the carbonyl of the nicotinamide ring of the NAD cofactor. The weaker InhA activity of 135809 compared with the other compounds with the most similar structures to it (see Figure 4 and Table S1 in the Supporting Information) might be due to these unfavorable electrostatic repulsions and perhaps to the less stable/less likely protonation state of the central thiadiazole ring (i.e., of the different independent models for the different protonation states of this compound that were screened, the model that passed the docking filters had a protonated thiadiazole, but ChemDraw calculations predict that this compound should not be protonated at neutral pH). 196166 was the least potent InhA inhibitor, and its docked mode displayed three unfavorable electrostatic repulsions with the phosphate adjacent to the ribose of the NAD cofactor. The terminal pyridine also displayed unfavorable electrostatic repulsion with the sulfur in the side chain of Met161, but the pyridine that is part of the two fused rings might T-stack with Phe149.

The eight inhibitors discovered were compared to a set of 157 previously characterized InhA inhibitors available in TB Mobile 2.<sup>111,112</sup> PCA showed that these eight InhA GO FAM inhibitors are generally not part of the main clusters of known InhA inhibitors but do have chemical properties similar to those



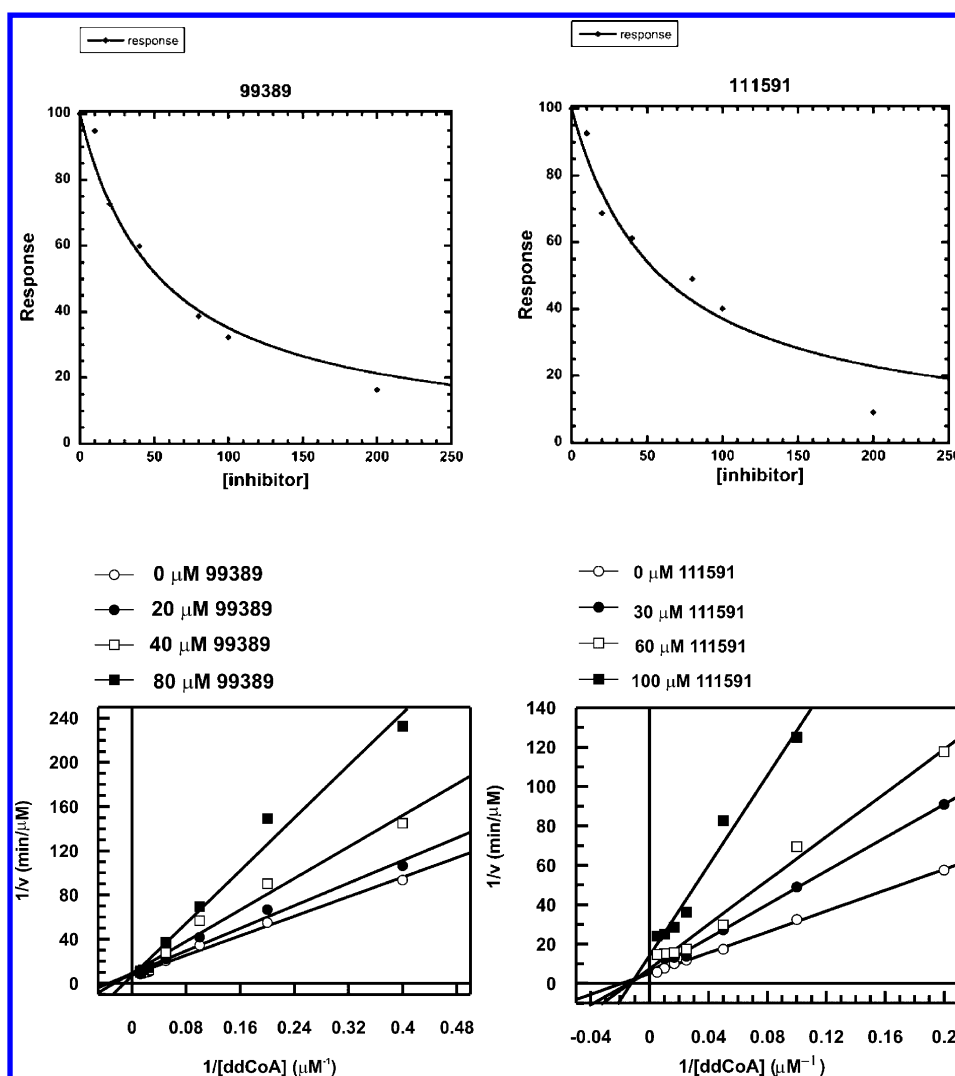


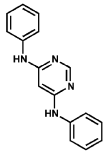
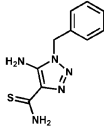
**Figure 6.** Kinetic data for the two most potent InhA inhibitors discovered, indicating that NCI 99389 is a competitive inhibitor and 111591 is noncompetitive.  $IC_{50}$  values were measured for the top two fragment hits, followed by a detailed mechanistic study to measure the  $K_i$  values. NCI 99389 showed a  $K_i^{app}$  of  $54.1 \pm 5.4 \mu M$  and a competitive binding mechanism, indicating that the inhibitor competed with the CoA substrate and bound directly to the enzyme. Conversely, NCI 111591 had a  $K_i^{app}$  of  $59.2 \pm 8.7 \mu M$  and a noncompetitive binding mechanism, suggesting a more complex scenario where the inhibitor could bind to both the holo enzyme and the substrate–enzyme complex.

of the known inhibitors (see Figure 5). Each inhibitor was also individually compared to all of the known InhA inhibitors in the TB Mobile data set to obtain sets of pairwise Tanimoto coefficients, which were then averaged (Table 2). Their average Tanimoto similarities ranged from 0.27 to 0.45 (with 1.0 indicating identical 2D structures). The two most promising new scaffolds discovered, NCI 99389 and 111591, had maximum Tanimoto similarities to known InhA inhibitors of 0.413 and 0.463, with minimum similarities of 0.146 and 0.131, and average similarity values of 0.309 and 0.368, respectively. These distinct cheminformatic analyses support these eight GO FAM compounds as novel InhA inhibitors on the basis of current literature data.

The top two fragment hits were then studied with (a) whole-cell *in vitro* *Mtb* growth experiments, using both the wild-type strain H37Rv and the *inhA*-overexpressing strain mc<sup>2</sup>4914,<sup>10</sup> and (b) Vero cell cytotoxicity experiments (see Table 3). Unfortunately, the top InhA inhibitor discovered, 99389, displayed a  $MIC_{90}$  of  $500 \mu M$  against wild-type *Mtb*. The  $MIC$  of  $>500 \mu M$  it exhibited against the *inhA*-overexpressing

strain of *Mtb* suggests that InhA might be the primary target against whole-cell *Mtb*. However, this compound lacked sufficient efficacy against *Mtb* and displayed considerable cytotoxicity with Vero cells, with a  $CC_{50}$  of  $<3.0 \mu M$ . As expected, the positive control INH displayed almost a 10-fold decrease in potency against the *inhA*-overexpressing strain, with  $MIC_{90}$  values of  $0.4 \mu M$  ( $0.05 \mu g/mL$ ) against wild-type *Mtb* and  $3 \mu M$  ( $0.4 \mu g/mL$ ) against strain mc<sup>2</sup>4914. The second most promising InhA inhibitor discovered, NCI 111591, displayed a  $MIC_{90}$  of  $125 \mu M$  against both wild-type *Mtb* and the *inhA*-overexpressing strain of *Mtb*. Although 111591 was 4-fold more potent against whole-cell *Mtb*, the lack of a shift in its potency against the *inhA*-overexpressing strain indicates that InhA is likely not its primary target in *Mtb*. In the PCA comparing the new inhibitors to the 157 known InhA inhibitors in TB Mobile 2,<sup>111,112</sup> 111591 was further from the main clusters of known InhA inhibitors, while 99389 was at the edge of the central cluster (see Figure 5). NCI 111591 was less toxic against Vero cells, with a  $CC_{50}$  of  $26 \mu M$ ; however, it still displayed an insufficient selectivity index of 0.21.

Table 3. Summary of Anti-*Mtb* Efficacies and Mammalian Cell Cytotoxicities

NCI ID	Structure	Vero cell cytotoxicity: CC <sub>50</sub> (μM)	MIC <sub>90</sub> vs <i>Mtb</i> (μM)	
			H37Rv wild type	mc <sup>2</sup> 4914 <i>inhA</i> overexpressor
99389		< 3.0	500	> 500
111591		26	125	125

Although several *InhA* inhibitors with nanomolar potency have been reported previously,<sup>11,15,41,125</sup> novel chemotypes that inhibit *InhA* are needed for the following reasons: (a) the presence of the phenol group in triclosan derivatives<sup>11,41,125</sup> poses a metabolic liability for in vivo applications;<sup>49–51</sup> (b) other advanced *InhA* leads have fared poorly when administered in mouse models of TB;<sup>15</sup> and (c) drug-resistant strains of *Mtb* (i.e., MDR-TB, XDR-TB, and TDR-TB) continue to evolve and spread throughout the world.<sup>1–7</sup> In addition, since 28–60% of TB cases are INH-resistant<sup>1,2,13</sup> and *InhA* is one of the most validated targets for treating TB, new chemotypes that inhibit *InhA* without displaying cross-resistance with INH could eventually seed the development of urgently needed new drug combinations for the treatment of active and latent TB infections.

The novel fragment hits we discovered against *InhA* displayed low-micromolar potency, with  $K_i$  values of 54.1 and 59.2 μM for the two most promising new scaffolds. With stringent criteria to define a hit (a  $K_i$  value <100 μM for a fragment-sized compound), this virtual screen had a 12.5% hit rate. Thus, from a computational chemistry perspective, this virtual screen was a success, since the median hit rate from hundreds of published virtual screens is ~13%.<sup>52</sup> More importantly, these novel *InhA* inhibitors are all predicted to base-stack with the NAD cofactor (instead of forming a covalent adduct with it). Our *InhA* inhibition assays demonstrated that these novel inhibitors do not require prior activation by *Mtb* KatG, which means that they should not be susceptible to the main mechanism of INH resistance found in clinical settings. In addition, the novel inhibitors discovered all lack the presence of the phenol group that poses a metabolic liability for triclosan derivatives. Consequently, the two most promising new chemotypes discovered might eventually enable the development of new *InhA* inhibitors that are effective against MDR-TB, XDR-TB, and TDR-TB. Since it is slightly weaker than NCI 99389, we consider NCI 111591 to be the second most promising new scaffold against *InhA* discovered in the present study. However, given its superior MIC against *Mtb* and its lower toxicity against Vero cells, NCI 111591 seems to be a more promising scaffold versus whole-cell *Mtb*.

Although these new chemotypes discovered against *InhA* are somewhat weak inhibitors (i.e., they are “fragment hits” and not drug-sized “leads”), they were identified from a diverse commercial library using freely available compounds. In addition, they are both fragment-sized compounds (i.e., MW < 300 g/mol).<sup>117</sup> Fragment-based hit discovery was not our initial goal, but it was the ultimate result of this pilot study. Unlike traditional high-throughput screens, fragment-based drug discovery is founded on screening a smaller number of smaller-sized compounds to advance the goal of discovering novel fragment hits with  $K_i$  or  $K_d$  values in the high-micromolar to low-millimolar range.<sup>118</sup> Those initial novel fragments can then be optimized using structure-based and medicinal chemistry strategies to develop potent leads, some of which have advanced to become clinical candidates<sup>117</sup> or FDA-approved drugs.<sup>126</sup> In the pioneering “SAR by NMR” study, the novel fragment hits discovered displayed  $K_d$  values of 100 μM to 9.5 mM.<sup>123</sup> Although a few studies have discovered fragment hits with potencies as great as 24 μM,<sup>127</sup> 49 μM,<sup>127</sup> 60 μM,<sup>127</sup> or 80 μM,<sup>128</sup> most fragment hits have potencies (i.e.,  $K_i$  or  $K_d$  values) in the 100–300 μM range, and many are in the low-millimolar range.<sup>87,117–119,121,122,127–129</sup> Thus, although our two fragment hits have very weak potencies compared with optimized lead compounds such as PT70, our hits have not yet been optimized against the *InhA* target or against whole-cell *Mtb*, and they are actually more potent than most novel fragment hits.

Our most promising new fragment hit against *InhA* has a fairly simple structure and should be amenable to structure-based, medicinal-chemistry-guided optimization. Because of their lack of whole-cell efficacy against *Mtb* and their inadequate selectivity indexes for Vero cell cytotoxicity, both of our top fragment hits will need considerable optimization before advancing to the lead compound stage. Several previous studies performed structure–activity relationship (SAR) experiments to guide the development of more potent *InhA* inhibitors.<sup>11,41,46,47,125</sup> Those studies suggest that our most promising new fragment hit could perhaps be developed into a more potent *InhA* inhibitor by appending appropriate functionality to one or both of the phenyl rings to make additional energetically favorable interactions with residues such as Gly96, Phe97, Phe149, Met155, Pro156, Ala157, Pro193, Ala198, Met199, Ile202, Val203, Leu207, Gln214, Ile215, or Leu218 or the NAD cofactor.

The similarity in the substructures that are predicted to base-stack with the NAD cofactor (see Figure 4) suggests that click chemistry, especially target-guided click chemistry,<sup>130–133</sup> might be a useful approach to aid the discovery and development of novel *InhA* inhibitors. Target-guided click chemistry is based on the principle that the azide- and alkyne-containing fragments will interact with each other and click together (to form the triazole ring) only if those fragments are correctly positioned and have high affinity and long residence times in the target enzyme.<sup>130–133</sup> Since inhibitors that display long residence times with pathogenic targets can have more favorable properties in vivo<sup>39,79–81,124</sup> and our computational results indicate that the triazole ring is predicted to form key base-stacking and hydrogen-bonding interactions with *InhA* (instead of just serving as a linker), we suggest that in situ click chemistry should be investigated in future studies against *InhA*.

## CONCLUSIONS

Our virtual screen of the NCI library with a published crystal structure (PDB ID 2X23<sup>39</sup>) led to the discovery of two promising and novel fragment hits that inhibit InhA activity. This pilot study has demonstrated the utility of the (public domain/open access) GO FAM docking data against InhA and of our approach to its analysis. Novel inhibitors of the key TB drug target InhA were discovered in an efficient manner, requiring the experimental assessment of fewer than 20 candidate compounds. These open access GO FAM data against InhA and other targets for treating TB and malaria represent a valuable resource for the drug discovery community.

## ASSOCIATED CONTENT

### Supporting Information

LC–MS and NMR data on the two fragment hits (Figures S1–S6), a Tanimoto comparison of each of the eight new inhibitors with the other seven inhibitors (Table S1), and a QuickTime animation of the predicted binding mode of the top InhA inhibitor discovered, NCI 99389 (video S1), made with PMV 1.5.6.<sup>83</sup> This material is available free of charge via the Internet at <http://pubs.acs.org>.

## AUTHOR INFORMATION

### Corresponding Author

\*Phone: (973) 972-0798. Fax: (973) 972-1141. E-mail: Alex.L.Perryman@rutgers.edu.

### Present Address

<sup>†</sup>A.L.P.: Rutgers University, NJMS-Medicine, Infectious Diseases, MSB I-503, 185 South Orange Avenue, Newark, NJ 07103.

### Author Contributions

<sup>○</sup>A.L.P. and W.Y. contributed equally.

### Notes

The authors declare no competing financial interest.

## ACKNOWLEDGMENTS

We are very grateful for the seed funding provided by the IBM International Foundation (from part of the prize money that Watson won on Jeopardy!), which was used to create the GO FAM project. This research was also funded in part by the “AutoDock Development and Maintenance” Grant to A.J.O. (R01 GM069832). We thank Sargis Dallakyan for maintaining the server that was used to submit these virtual screens to the GO FAM project and to receive the results from it. We thank the IBM World Community Grid team (including Juan A. Hindo, Viktors Berstis, Al Seippel, Keith J. Uplinger, Kevin Reed, Tedi Hahn, Jonathan D. Armstrong, and Erika Tuttle) for devoting their time to this humanitarian effort. We are also grateful for the World Community Grid volunteers, who donated their CPU time to support the GO FAM calculations. All of the GO FAM results are legally public domain and thus are accessible to any scientist by contacting A.J.O. or A.L.P. We thank the Developmental Therapeutics Program, Division of Cancer Treatment and Diagnosis, National Cancer Institute, National Institutes of Health (NIH), an agency of the U.S. Public Health Service (PHS), for providing free access to these NCI compounds. We thank Thomas Mayo and Katalin Nadassy of Biovia for providing free access to and assistance with Discovery Studio and Pipeline Pilot. J.S.F. is grateful to Professor Bill Jacobs (Albert Einstein College of Medicine) for

his lab’s kind gift of *M. tuberculosis* strain mc<sup>2</sup>4914. TB Mobile was partially funded by Award 2R42AI088893-02 “Identification of Novel Therapeutics for Tuberculosis Combining Cheminformatics, Diverse Databases and Logic Based Pathway Analysis” to S.E. from the National Institute of Allergy and Infectious Diseases, NIH. Funding was also provided in part by NIH 3DP2OD008459-01S1 to J.S.F. and GM102864 to P.J.T.

## REFERENCES

- (1) *Global Tuberculosis Report*; World Health Organization: Geneva, 2013.
- (2) Abubakar, I.; Zignol, M.; Falzon, D.; Ravigliione, M.; Ditiu, L.; Masham, S.; Adetifa, I.; Ford, N.; Cox, H.; Lawn, S. D.; Marais, B. J.; McHugh, T. D.; Mwaba, P.; Bates, M.; Lipman, M.; Zijenah, L.; Logan, S.; McNerney, R.; Zumla, A.; Sarda, K.; Nahid, P.; Hoelscher, M.; Pletschette, M.; Memish, Z. A.; Kim, P.; Hafner, R.; Cole, S.; Migliori, G. B.; Maeurer, M.; Schito, M.; Zumla, A. Drug-Resistant Tuberculosis: Time for Visionary Political Leadership. *Lancet Infect. Dis.* **2013**, *13*, 529–39.
- (3) Velayati, A. A.; Farnia, P.; Masjedi, M. R. The Totally Drug Resistant Tuberculosis (TDR-TB). *Int. J. Clin. Exp. Med.* **2013**, *6*, 307–9.
- (4) Dheda, K.; Migliori, G. B. The Global Rise of Extensively Drug-Resistant Tuberculosis: Is the Time To Bring Back Sanatoria Now Overdue? *Lancet* **2012**, *379*, 773–5.
- (5) Gothi, D.; Joshi, J. M. Resistant TB: Newer Drugs and Community Approach. *Recent Pat. Anti-Infect. Drug Discovery* **2011**, *6*, 27–37.
- (6) Udawadia, Z. F.; Amale, R. A.; Ajbani, K. K.; Rodrigues, C. Totally Drug-Resistant Tuberculosis in India. *Clin. Infect. Dis.* **2012**, *54*, 579–81.
- (7) Velayati, A. A.; Masjedi, M. R.; Farnia, P.; Tabarsi, P.; Ghanavi, J.; ZiaZarifi, A. H.; Hoffner, S. E. Emergence of New Forms of Totally Drug-Resistant Tuberculosis Bacilli: Super Extensively Drug-Resistant Tuberculosis or Totally Drug-Resistant Strains in Iran. *CHEST J.* **2009**, *136*, 420–5.
- (8) Shah, N. S.; Richardson, J.; Moodley, P.; Babaria, P.; Ramtahal, M.; Heyssel, S. K.; Li, X.; Moll, A. P.; Friedland, G.; Sturm, A. W.; Gandhi, N. R. Increasing Drug Resistance in Extensively Drug-Resistant Tuberculosis, South Africa. *Emerging Infect. Dis.* **2011**, *17*, 510–3.
- (9) Vilcheze, C.; Jacobs, W. R., Jr. The Mechanism of Isoniazid Killing: Clarity through the Scope of Genetics. *Annu. Rev. Microbiol.* **2007**, *61*, 35–50.
- (10) Vilcheze, C.; Wang, F.; Arai, M.; Hazbon, M. H.; Colangeli, R.; Kremer, L.; Weisbrod, T. R.; Alland, D.; Sacchettini, J. C.; Jacobs, W. R. Transfer of a Point Mutation in *Mycobacterium tuberculosis* InhA Resolves the Target of Isoniazid. *Nat. Med.* **2006**, *12*, 1027–29.
- (11) Freundlich, J. S.; Wang, F.; Vilcheze, C.; Gulten, G.; Langley, R.; Schiehsler, G. A.; Jacobus, D. P.; Jacobs, W. R.; Sacchettini, J. C. Triclosan Derivatives: Towards Potent Inhibitors of Drug-Sensitive and Drug-Resistant *Mycobacterium tuberculosis*. *ChemMedChem* **2009**, *4*, 241–8.
- (12) North, E. J.; Jackson, M.; Lee, R. E. New Approaches To Target the Mycolic Acid Biosynthesis Pathway for the Development of Tuberculosis Therapeutics. *Curr. Pharm. Des.* **2014**, *20*, 4357–78.
- (13) Vilcheze, C.; Baughn, A. D.; Tufariello, J.; Leung, L. W.; Kuo, M.; Basler, C. F.; Alland, D.; Sacchettini, J. C.; Freundlich, J. S.; Jacobs, W. R., Jr. Novel Inhibitors of InhA Efficiently Kill *Mycobacterium tuberculosis* under Aerobic and Anaerobic Conditions. *Antimicrob. Agents Chemother.* **2011**, *55*, 3889–98.
- (14) Heym, B.; Zhang, Y.; Poulet, S.; Young, D.; Cole, S. T. Characterization of the KatG Gene Encoding a Catalase-Peroxidase Required for the Isoniazid Susceptibility of *Mycobacterium tuberculosis*. *J. Bacteriol.* **1993**, *175*, 4255–9.
- (15) Encinas, L.; O’Keefe, H.; Neu, M.; Remuinan, M. J.; Patel, A. M.; Guardia, A.; Davie, C. P.; Perez-Macias, N.; Yang, H.; Convery, M. A.; Messer, J. A.; Perez-Herran, E.; Centrella, P. A.; Alvarez-Gomez,



- D.; Clark, M. A.; Huss, S.; O'Donovan, G. K.; Ortega-Muro, F.; McDowell, W.; Castaneda, P.; Arico-Muendel, C. C.; Pajk, S.; Rullas, J.; Angulo-Barturen, I.; Alvarez-Ruiz, E.; Mendoza-Losana, A.; Pages, L. B.; Castro-Pichel, J.; Evindar, G. Encoded Library Technology as a Source of Hits for the Discovery and Lead Optimization of a Potent and Selective Class of Bactericidal Direct Inhibitors of *Mycobacterium tuberculosis* InhA. *J. Med. Chem.* **2014**, *57*, 1276–88.
- (16) Zhang, L.; Ye, Y.; Duo, L.; Wang, T.; Song, X.; Lu, X.; Ying, B.; Wang, L. Application of Genotype MTBDRplus in Rapid Detection of the *Mycobacterium tuberculosis* Complex as Well as Its Resistance to Isoniazid and Rifampin in a High Volume Laboratory in Southern China. *Mol. Biol. Rep.* **2011**, *38*, 2185–92.
- (17) Tonge, P. J.; Kisker, C.; Slayden, R. A. Development of Modern InhA Inhibitors To Combat Drug Resistant Strains of *Mycobacterium tuberculosis*. *Curr. Top. Med. Chem.* **2007**, *7*, 489–98.
- (18) Hazbon, M. H.; Brimacombe, M.; Bobadilla del Valle, M.; Cavatore, M.; Guerrero, M. I.; Varma-Basil, M.; Billman-Jacobe, H.; Lavender, C.; Fyfe, J.; Garcia-Garcia, L.; Leon, C. I.; Bose, M.; Chaves, F.; Murray, M.; Eisenach, K. D.; Sifuentes-Osornio, J.; Cave, M. D.; Ponce de Leon, A.; Alland, D. Population Genetics Study of Isoniazid Resistance Mutations and Evolution of Multidrug-Resistant *Mycobacterium tuberculosis*. *Antimicrob. Agents Chemother.* **2006**, *50*, 2640–9.
- (19) Ajbani, K.; Rodrigues, C.; Shenai, S.; Mehta, A. Mutation Detection and Accurate Diagnosis of Extensively Drug-Resistant Tuberculosis: Report from a Tertiary Care Center in India. *J. Clin. Microbiol.* **2011**, *49*, 1588–90.
- (20) Chia, B.-S.; Lanzas, F.; Rifat, D.; Herrera, A.; Kim, E. Y.; Sailer, C.; Torres-Chavolla, E.; Narayanaswamy, P.; Einarsson, V.; Bravo, J.; Pascuale, J. M.; Ioerger, T. R.; Sacchettini, J. C.; Karakousis, P. C. Use of Multiplex Allele-Specific Polymerase Chain Reaction (MAS-PCR) To Detect Multidrug-Resistant Tuberculosis in Panama. *PLoS One* **2012**, *7*, No. e40456.
- (21) Fenner, L.; Egger, M.; Bodmer, T.; Altpeter, E.; Zwahlen, M.; Jaton, K.; Pfyffer, G. E.; Borrell, S.; Dubuis, O.; Bruderer, T.; Siegrist, H. H.; Furrer, H.; Calmy, A.; Fehr, J.; Stalder, J. M.; Ninet, B.; Bottger, E. C.; Gagneux, S. Effect of Mutation and Genetic Background on Drug Resistance in *Mycobacterium tuberculosis*. *Antimicrob. Agents Chemother.* **2012**, *56*, 3047–53.
- (22) Tessema, B.; Beer, J.; Emmrich, F.; Sack, U.; Rodloff, A. C. Analysis of Gene Mutations Associated with Isoniazid, Rifampicin and Ethambutol Resistance among *Mycobacterium tuberculosis* Isolates from Ethiopia. *BMC Infect. Dis.* **2012**, *12*, No. 37.
- (23) Shubladze, N.; Tadumadze, N.; Bablshvili, N. Molecular Patterns of Multidrug Resistance of *Mycobacterium tuberculosis* in Georgia. *Int. J. Mycobacteriol.* **2013**, *2*, 73–8.
- (24) Hung, N. V.; Ando, H.; Thuy, T. T.; Kuwahara, T.; Hang, N. T.; Sakurada, S.; Thuong, P. H.; Lien, L. T.; Keicho, N. Clonal Expansion of *Mycobacterium tuberculosis* Isolates and Coexisting Drug Resistance in Patients Newly Diagnosed with Pulmonary Tuberculosis in Hanoi, Vietnam. *BMC Res. Notes* **2013**, *6*, No. 444.
- (25) Tseng, S. T.; Tai, C. H.; Li, C. R.; Lin, C. F.; Shi, Z. Y. The Mutations of KatG and InhA Genes of Isoniazid-Resistant *Mycobacterium tuberculosis* Isolates in Taiwan. *J. Microbiol. Immunol. Infect.* **2013**, 163–71.
- (26) Huyen, M. N.; Cobelens, F. G.; Buu, T. N.; Lan, N. T.; Dung, N. H.; Kremer, K.; Tiemersma, E. W.; van Soolingen, D. Epidemiology of Isoniazid Resistance Mutations and Their Effect on Tuberculosis Treatment Outcomes. *Antimicrob. Agents Chemother.* **2013**, *57*, 3620–7.
- (27) Yadav, R.; Sethi, S.; Dhatwalia, S. K.; Gupta, D.; Mewara, A.; Sharma, M. Molecular Characterisation of Drug Resistance in *Mycobacterium tuberculosis* Isolates from North India. *Int. J. Tuberc. Lung Dis.* **2013**, *17*, 251–7.
- (28) Varghese, B.; Hillemann, A.; Wijayanti, D. R.; Shoukri, M.; Al-Rabiah, F.; Al-Omari, R.; Al-Hajjo, S. New Insight into the Molecular Characterization of Isoniazid and Rifampicin Resistant *Mycobacterium tuberculosis* Strains from Saudi Arabia. *Infect. Genet. Evol.* **2012**, *12*, 549–56.
- (29) Ali, A.; Hasan, R.; Jabeen, K.; Jabeen, N.; Qadeer, E.; Hasan, Z. Characterization of Mutations Conferring Extensive Drug Resistance to *Mycobacterium tuberculosis* Isolates in Pakistan. *Antimicrob. Agents Chemother.* **2011**, *55*, 5654–9.
- (30) Balabanova, Y.; Nikolayevskyy, V.; Ignatyeva, O.; Kontsevaya, I.; Rutterford, C. M.; Shakhmistova, A.; Malomanova, N.; Chinkova, Y.; Mironova, S.; Fedorin, I.; Drobniewski, F. A. Survival of Civilian and Prisoner Drug-Sensitive, Multi- and Extensive Drug-Resistant Tuberculosis Cohorts Prospectively Followed in Russia. *PLoS One* **2011**, *6*, No. e20531.
- (31) Kozhamkulov, U.; Akhmetova, A.; Rakhimova, S.; Belova, E.; Alenova, A.; Bismilda, V.; Chingissova, L.; Ismailov, S.; Ramanculov, E.; Momynaliev, K. Molecular Characterization of Rifampicin- and Isoniazid-Resistant *Mycobacterium tuberculosis* Strains Isolated in Kazakhstan. *Jpn. J. Infect. Dis.* **2011**, *64*, 253–5.
- (32) Dias, M. V.; Vasconcelos, I. B.; Prado, A. M.; Fadel, V.; Basso, L. A.; de Azevedo, W. F., Jr.; Santos, D. S. Crystallographic Studies on the Binding of Isonicotinyl-NAD Adduct to Wild-Type and Isoniazid Resistant 2-*trans*-Enoyl-ACP (CoA) Reductase from *Mycobacterium tuberculosis*. *J. Struct. Biol.* **2007**, *159*, 369–80.
- (33) He, X.; Alian, A.; Stroud, R.; Ortiz de Montellano, P. R. Pyrrolidine Carboxamides as a Novel Class of Inhibitors of Enoyl Acyl Carrier Protein Reductase from *Mycobacterium tuberculosis*. *J. Med. Chem.* **2006**, *49*, 6308–23.
- (34) Oliveira, J. S.; Pereira, J. H.; Canduri, F.; Rodrigues, N. C.; de Souza, O. N.; de Azevedo, W. F., Jr.; Basso, L. A.; Santos, D. S. Crystallographic and Pre-Steady-State Kinetics Studies on Binding of NADH to Wild-Type and Isoniazid-Resistant Enoyl-ACP (CoA) Reductase Enzymes from *Mycobacterium tuberculosis*. *J. Mol. Biol.* **2006**, *359*, 646–66.
- (35) Shirude, P. S.; Madhavapeddi, P.; Naik, M.; Murugan, K.; Shinde, V.; Nandishaiah, R.; Bhat, J.; Kumar, A.; Hameed, S.; Holdgate, G.; Davies, G.; McMiken, H.; Hegde, N.; Ambady, A.; Venkatraman, J.; Panda, M.; Bhandodkar, B.; Sambandamurthy, V. K.; Read, J. A. Methyl-Thiazoles: A Novel Mode of Inhibition with the Potential To Develop Novel Inhibitors Targeting InhA in *Mycobacterium tuberculosis*. *J. Med. Chem.* **2013**, *56*, 8533–42.
- (36) Wang, F.; Langley, R.; Gulten, G.; Dover, L. G.; Besra, G. S.; Jacobs, W. R., Jr.; Sacchettini, J. C. Mechanism of Thioamide Drug Action against Tuberculosis and Leprosy. *J. Exp. Med.* **2007**, *204*, 73–8.
- (37) Rozwarski, D. A.; Vilcheze, C.; Sugantino, M.; Bittman, R.; Sacchettini, J. C. Crystal Structure of the *Mycobacterium tuberculosis* Enoyl-ACP Reductase, InhA, in Complex with NAD<sup>+</sup> and a C<sub>16</sub> Fatty Acyl Substrate. *J. Biol. Chem.* **1999**, *274*, 15582–9.
- (38) Rozwarski, D. A.; Grant, G. A.; Barton, D. H.; Jacobs, W. R., Jr.; Sacchettini, J. C. Modification of the NADH of the Isoniazid Target (InhA) from *Mycobacterium tuberculosis*. *Science* **1998**, *279*, 98–102.
- (39) Luckner, S. R.; Liu, N.; am Ende, C. W.; Tonge, P. J.; Kisker, C. A Slow, Tight Binding Inhibitor of InhA, the Enoyl-Acyl Carrier Protein Reductase from *Mycobacterium tuberculosis*. *J. Biol. Chem.* **2010**, *285*, 14330–7.
- (40) He, X.; Alian, A.; Ortiz de Montellano, P. R. Inhibition of the *Mycobacterium tuberculosis* Enoyl Acyl Carrier Protein Reductase InhA by Arylamides. *Bioorg. Med. Chem.* **2007**, *15*, 6649–58.
- (41) Sullivan, T. J.; Truglio, J. J.; Boyne, M. E.; Novichenok, P.; Zhang, X.; Stratton, C. F.; Li, H. J.; Kaur, T.; Amin, A.; Johnson, F.; Slayden, R. A.; Kisker, C.; Tonge, P. J. High Affinity InhA Inhibitors with Activity against Drug-Resistant Strains of *Mycobacterium tuberculosis*. *ACS Chem. Biol.* **2006**, *1*, 43–53.
- (42) Hartkoorn, R. C.; Sala, C.; Neres, J.; Pojer, F.; Magnet, S.; Mukherjee, R.; Uplekar, S.; Boy-Rottger, S.; Altmann, K. H.; Cole, S. T. Towards a New Tuberculosis Drug: Pyridomycin—Nature's Isoniazid. *EMBO Mol. Med.* **2012**, *4*, 1032–42.
- (43) Hartkoorn, R. C.; Pojer, F.; Read, J. A.; Gingell, H.; Neres, J.; Horlacher, O. P.; Altmann, K. H.; Cole, S. T. Pyridomycin Bridges the NADH- and Substrate-Binding Pockets of the Enoyl Reductase InhA. *Nat. Chem. Biol.* **2014**, *10*, 96–8.

- (44) Argyrou, A.; Vetting, M. W.; Blanchard, J. S. New Insight into the Mechanism of Action of and Resistance to Isoniazid: Interaction of *Mycobacterium tuberculosis* Enoyl-ACP Reductase with INH–NADP. *J. Am. Chem. Soc.* **2007**, *129*, 9582–3.
- (45) Pan, P.; Tonge, P. J. Targeting InhA, the FASII Enoyl-Acp Reductase: SAR Studies on Novel Inhibitor Scaffolds. *Curr. Top. Med. Chem.* **2012**, *12*, 672–93.
- (46) Boyne, M. E.; Sullivan, T. J.; am Ende, C. W.; Lu, H.; Gruppo, V.; Heaslip, D.; Amin, A. G.; Chatterjee, D.; Lenaerts, A.; Tonge, P. J.; Slayden, R. A. Targeting Fatty Acid Biosynthesis for the Development of Novel Chemotherapeutics against *Mycobacterium tuberculosis*: Evaluation of A-Ring-Modified Diphenyl Ethers as High-Affinity InhA Inhibitors. *Antimicrob. Agents Chemother.* **2007**, *51*, 3562–7.
- (47) Kuo, M. R.; Morbidoni, H. R.; Alland, D.; Sneddon, S. F.; Gourlie, B. B.; Staveski, M. M.; Leonard, M.; Gregory, J. S.; Janjigian, A. D.; Yee, C.; Musser, J. M.; Kreiswirth, B.; Iwamoto, H.; Perozzo, R.; Jacobs, W. R., Jr.; Sacchettini, J. C.; Fidock, D. A. Targeting Tuberculosis and Malaria through Inhibition of Enoyl Reductase: Compound Activity and Structural Data. *J. Biol. Chem.* **2003**, *278*, 20851–9.
- (48) Lu, H.; Tonge, P. J. Inhibitors of FabI, an Enzyme Drug Target in the Bacterial Fatty Acid Biosynthesis Pathway. *Acc. Chem. Res.* **2008**, *41*, 11–20.
- (49) England, K.; am Ende, C.; Lu, H.; Sullivan, T. J.; Marlenee, N. L.; Bowen, R. A.; Knudson, S. E.; Knudson, D. L.; Tonge, P. J.; Slayden, R. A. Substituted Diphenyl Ethers as a Broad-Spectrum Platform for the Development of Chemotherapeutics for the Treatment of Tularaemia. *J. Antimicrob. Chemother.* **2009**, *64*, 1052–61.
- (50) Wu, J. L.; Liu, J.; Cai, Z. Determination of Triclosan Metabolites by Using In-Source Fragmentation from High-Performance Liquid Chromatography/Negative Atmospheric Pressure Chemical Ionization Ion Trap Mass Spectrometry. *Rapid Commun. Mass Spectrom.* **2010**, *24*, 1828–34.
- (51) Wang, L. Q.; Falany, C. N.; James, M. O. Triclosan as a Substrate and Inhibitor of 3'-Phosphoadenosine 5'-Phosphosulfate-Sulfotransferase and UDP-Glucuronosyl Transferase in Human Liver Fractions. *Drug Metab. Dispos.* **2004**, *32*, 1162–9.
- (52) Zhu, T.; Cao, S.; Su, P.-C.; Patel, R.; Shah, D.; Chokshi, H. B.; Szukala, R.; Johnson, M. E.; Hevener, K. E. Hit Identification and Optimization in Virtual Screening: Practical Recommendations Based on a Critical Literature Analysis. *J. Med. Chem.* **2013**, *56*, 6560–72.
- (53) Tanrikulu, Y.; Kruger, B.; Proschak, E. The Holistic Integration of Virtual Screening in Drug Discovery. *Drug Discovery Today* **2013**, *18*, 358–64.
- (54) Goodsell, D. S.; Olson, A. J. Automated Docking of Substrates to Proteins by Simulated Annealing. *Proteins* **1990**, *8*, 195–202.
- (55) Goodsell, D. S.; Lauble, H.; Stout, C. D.; Olson, A. J. Automated Docking in Crystallography: Analysis of the Substrates of Aconitase. *Proteins* **1993**, *17*, 1–10.
- (56) Goodsell, D. S.; Morris, G. M.; Olson, A. J. Automated Docking of Flexible Ligands: Applications of Autodock. *J. Mol. Recognit.* **1996**, *9*, 1–5.
- (57) Morris, G. M.; Goodsell, D. S.; Huey, R.; Olson, A. J. Distributed Automated Docking of Flexible Ligands to Proteins: Parallel Applications of Autodock 2.4. *J. Comput.-Aided. Mol. Des.* **1996**, *10*, 293–304.
- (58) Olson, A. J.; Goodsell, D. S. Automated Docking and the Search for HIV Protease Inhibitors. *SAR QSAR Environ. Res.* **1998**, *8*, 273–85.
- (59) Soares, T. A.; Goodsell, D. S.; Briggs, J. M.; Ferreira, R.; Olson, A. J. Docking of 4-Oxalocrotonate Tautomerase Substrates: Implications for the Catalytic Mechanism. *Biopolymers* **1999**, *50*, 319–28.
- (60) Osterberg, F.; Morris, G. M.; Sanner, M. F.; Olson, A. J.; Goodsell, D. S. Automated Docking to Multiple Target Structures: Incorporation of Protein Mobility and Structural Water Heterogeneity in Autodock. *Proteins* **2002**, *46*, 34–40.
- (61) Trott, O.; Olson, A. J. Autodock Vina: Improving the Speed and Accuracy of Docking with a New Scoring Function, Efficient Optimization, and Multithreading. *J. Comput. Chem.* **2010**, *31*, 455–61.
- (62) Kumar, M.; Vijayakrishnan, R.; Subba Rao, G. In Silico Structure-Based Design of a Novel Class of Potent and Selective Small Peptide Inhibitor of *Mycobacterium tuberculosis* Dihydrofolate Reductase, a Potential Target for Anti-TB Drug Discovery. *Mol. Diversity* **2010**, *14*, 595–604.
- (63) Kumar, A.; Siddiqi, M. I. Virtual Screening against *Mycobacterium tuberculosis* Dihydrofolate Reductase: Suggested Workflow for Compound Prioritization Using Structure Interaction Fingerprints. *J. Mol. Graphics Modell.* **2008**, *27*, 476–88.
- (64) Lu, X. Y.; Chen, Y. D.; Jiang, Y. J.; You, Q. D. Discovery of Potential New InhA Direct Inhibitors Based on Pharmacophore and 3D-QSAR Analysis Followed by in Silico Screening. *Eur. J. Med. Chem.* **2009**, *44*, 3718–30.
- (65) Lu, X. Y.; Chen, Y. D.; You, Q. D. 3D-QSAR Studies of Arylcarboxamides with Inhibitory Activity on InhA Using Pharmacophore-Based Alignment. *Chem. Biol. Drug Des.* **2010**, *75*, 195–203.
- (66) Subba Rao, G.; Vijayakrishnan, R.; Kumar, M. Structure-Based Design of a Novel Class of Potent Inhibitors of InhA, the Enoyl Acyl Carrier Protein Reductase from *Mycobacterium tuberculosis*: A Computer Modelling Approach. *Chem. Biol. Drug Des.* **2008**, *72*, 444–9.
- (67) Punkvang, A.; Saparpakorn, P.; Hannongbua, S.; Wolschann, P.; Pungpo, P. Elucidating Drug–Enzyme Interactions and Their Structural Basis for Improving the Affinity and Potency of Isoniazid and Its Derivatives Based on Computer Modeling Approaches. *Molecules* **2010**, *15*, 2791–813.
- (68) Kinnings, S. L.; Liu, N.; Tonge, P. J.; Jackson, R. M.; Xie, L.; Bourne, P. E. A Machine Learning-Based Method To Improve Docking Scoring Functions and Its Application to Drug Repurposing. *J. Chem. Inf. Model.* **2011**, *51*, 408–19.
- (69) Pauli, I.; dos Santos, R. N.; Rostirolla, D. C.; Martinelli, L. K.; Ducati, R. G.; Timmers, L. F.; Basso, L. A.; Santos, D. S.; Guido, R. V.; Andricopulo, A. D.; de Souza, O. N. Discovery of New Inhibitors of *Mycobacterium tuberculosis* InhA Enzyme Using Virtual Screening and a 3D-Pharmacophore-Based Approach. *J. Chem. Inf. Model.* **2013**, *53*, 2390–401.
- (70) Mohan, S. B.; Ravi Kumar, B. V.; Dinda, S. C.; Naik, D.; Prabu Seenivasan, S.; Kumar, V.; Rana, D. N.; Brahmksatriya, P. S. Microwave-Assisted Synthesis, Molecular Docking and Antitubercular Activity of 1,2,3,4-Tetrahydropyrimidine-5-carbonitrile Derivatives. *Bioorg. Med. Chem. Lett.* **2012**, *22*, 7539–42.
- (71) Muddassar, M.; Jang, J. W.; Hong, S. K.; Cho, Y. S.; Kim, E. E.; Keum, K. C.; Oh, T.; Cho, S. N.; Pae, A. N. Identification of Novel Antitubercular Compounds through Hybrid Virtual Screening Approach. *Bioorg. Med. Chem.* **2010**, *18*, 6914–21.
- (72) Izumizono, Y.; Arevalo, S.; Koseki, Y.; Kuroki, M.; Aoki, S. Identification of Novel Potential Antibiotics for Tuberculosis by in Silico Structure-Based Drug Screening. *Eur. J. Med. Chem.* **2011**, *46*, 1849–56.
- (73) Kinjo, T.; Koseki, Y.; Kobayashi, M.; Yamada, A.; Morita, K.; Yamaguchi, K.; Tsurusawa, R.; Gulten, G.; Komatsu, H.; Sakamoto, H.; Sacchettini, J. C.; Kitamura, M.; Aoki, S. Identification of Compounds with Potential Antibacterial Activity against *Mycobacterium tuberculosis* through Structure-Based Drug Screening. *J. Chem. Inf. Model.* **2013**, *53*, 1200–12.
- (74) Perryman, A. L., I'll Take "Curing Malaria" for \$1,000, Alex. Citizen IBM Blog, November 2011. <http://citizenibm.com/2011/11> (accessed Nov 7, 2014).
- (75) Perryman, A. L. GO Fight Against Malaria: Project Overview. <http://www.worldcommunitygrid.org/research/gfam/overview.do> (accessed Nov 7, 2014).
- (76) Perryman, A. L.; Olson, A. J. Global Online Fight Against Malaria Project. <http://GOFightAgainstMalaria.scripps.edu> (accessed Nov 7, 2014).
- (77) Irwin, J. J.; Shoichet, B. K. ZINC—A Free Database of Commercially Available Compounds for Virtual Screening. *J. Chem. Inf. Model.* **2005**, *45*, 177–82.



- (78) Stec, J.; Vilcheze, C.; Lun, S.; Perryman, A. L.; Wang, X.; Freundlich, J. S.; Bishai, W.; Jacobs, W. R., Jr.; Kozikowski, A. P. Biological Evaluation of Potent Triclosan-Derived Inhibitors of the Enoyl-Acyl Carrier Protein Reductase InhA in Drug-Sensitive and Drug-Resistant Strains of *Mycobacterium tuberculosis*. *ChemMedChem* **2014**, *9*, 2528–37.
- (79) Chang, A.; Schiebel, J.; Yu, W.; Bommineni, G. R.; Pan, P.; Baxter, M. V.; Khanna, A.; Sottriffer, C. A.; Kisker, C.; Tonge, P. J. Rational Optimization of Drug–Target Residence Time: Insights from Inhibitor Binding to the *Staphylococcus aureus* FabI Enzyme–Product Complex. *Biochemistry* **2013**, *52*, 4217–28.
- (80) Lu, H.; Tonge, P. J. Drug–Target Residence Time: Critical Information for Lead Optimization. *Curr. Opin. Chem. Biol.* **2010**, *14*, 467–74.
- (81) Lu, H.; England, K.; am Ende, C.; Truglio, J. J.; Luckner, S.; Reddy, B. G.; Marlenee, N. L.; Knudson, S. E.; Knudson, D. L.; Bowen, R. A.; Kisker, C.; Slayden, R. A.; Tonge, P. J. Slow-Onset Inhibition of the FabI Enoyl Reductase from *Francisella tularensis*: Residence Time and in Vivo Activity. *ACS Chem. Biol.* **2009**, *4*, 221–31.
- (82) Chen, V. B.; Arendall, W. B., III; Headd, J. J.; Keedy, D. A.; Immormino, R. M.; Kapral, G. J.; Murray, L. W.; Richardson, J. S.; Richardson, D. C. Molprobity: All-Atom Structure Validation for Macromolecular Crystallography. *Acta Crystallogr., Sect. D: Biol. Crystallogr.* **2010**, *66*, 12–21.
- (83) Morris, G. M.; Huey, R.; Lindstrom, W.; Sanner, M. F.; Belew, R. K.; Goodsell, D. S.; Olson, A. J. Autodock4 and Autodocktools4: Automated Docking with Selective Receptor Flexibility. *J. Comput. Chem.* **2009**, *30*, 2785–91.
- (84) Forli, S.; Olson, A. J. *Raccoon*; Molecular Graphics Laboratory: La Jolla, CA, 2010.
- (85) Cosconati, S.; Forli, S.; Perryman, A. L.; Harris, R.; Goodsell, D. S.; Olson, A. J. Virtual Screening with Autodock: Theory and Practice. *Expert Opin. Drug Discovery* **2010**, *5*, 597–607.
- (86) Perryman, A. L.; Santiago, D. N.; Forli, S.; Santos-Martins, D.; Olson, A. J. Virtual Screening with Autodock Vina and the Common Pharmacophore Engine of a Low Diversity Library of Fragments and Hits against the Three Allosteric Sites of HIV Integrase: Participation in the SAMPL4 Protein–Ligand Binding Challenge. *J. Comput.-Aided Mol. Des.* **2014**, *28*, 429–41.
- (87) Mobley, D. L.; Liu, S.; Lim, N. M.; Wymer, K. L.; Perryman, A. L.; Forli, S.; Deng, N.; Su, J.; Branson, K.; Olson, A. J. Blind Prediction of HIV Integrase Binding from the SAMPL4 Challenge. *J. Comput.-Aided Mol. Des.* **2014**, *28*, 327–45.
- (88) Voet, A. R.; Kumar, A.; Berenger, F.; Zhang, K. Y. Combining in Silico and in Cerebro Approaches for Virtual Screening and Pose Prediction in SAMPL4. *J. Comput.-Aided Mol. Des.* **2014**, *28*, 363–73.
- (89) Lipinski, C. A.; Lombardo, F.; Dominy, B. W.; Feeney, P. J. Experimental and Computational Approaches To Estimate Solubility and Permeability in Drug Discovery and Development Settings. *Adv. Drug Delivery Rev.* **2001**, *46*, 3–26.
- (90) Hunter, C. A. Sequence-Dependent DNA Structure. The Role of Base Stacking Interactions. *J. Mol. Biol.* **1993**, *230*, 1025–54.
- (91) Jiang, X.; Loo, D. D.; Hirayama, B. A.; Wright, E. M. The Importance of Being Aromatic:  $\pi$  Interactions in Sodium Symporters. *Biochemistry* **2012**, *51*, 9480–7.
- (92) Durrant, J. D.; McCammon, J. A. BINANA: A Novel Algorithm for Ligand-Binding Characterization. *J. Mol. Graphics Modell.* **2011**, *29*, 888–93.
- (93) Sponer, J.; Leszczynski, J.; Hobza, P. Electronic Properties, Hydrogen Bonding, Stacking, and Cation Binding of DNA and RNA Bases. *Biopolymers* **2001**, *61*, 3–31.
- (94) Lefebvre, E.; Schiffer, C. A. Resilience to Resistance of HIV-1 Protease Inhibitors: Profile of Darunavir. *AIDS Rev.* **2008**, *10*, 131–42.
- (95) Nalam, M. N.; Ali, A.; Altman, M. D.; Reddy, G. S.; Chellappan, S.; Kairys, V.; Ozen, A.; Cao, H.; Gilson, M. K.; Tidor, B.; Rana, T. M.; Schiffer, C. A. Evaluating the Substrate-Envelope Hypothesis: Structural Analysis of Novel HIV-1 Protease Inhibitors Designed To Be Robust against Drug Resistance. *J. Virol.* **2010**, *84*, 5368–78.
- (96) Kairys, V.; Gilson, M. K.; Lather, V.; Schiffer, C. A.; Fernandes, M. X. Toward the Design of Mutation-Resistant Enzyme Inhibitors: Further Evaluation of the Substrate Envelope Hypothesis. *Chem. Biol. Drug Des.* **2009**, *74*, 234–45.
- (97) Altman, M. D.; Ali, A.; Reddy, G. S.; Nalam, M. N.; Anjum, S. G.; Cao, H.; Chellappan, S.; Kairys, V.; Fernandes, M. X.; Gilson, M. K.; Schiffer, C. A.; Rana, T. M.; Tidor, B. HIV-1 Protease Inhibitors from Inverse Design in the Substrate Envelope Exhibit Subnanomolar Binding to Drug-Resistant Variants. *J. Am. Chem. Soc.* **2008**, *130*, 6099–113.
- (98) Chellappan, S.; Kiran Kumar Reddy, G. S.; Ali, A.; Nalam, M. N.; Anjum, S. G.; Cao, H.; Kairys, V.; Fernandes, M. X.; Altman, M. D.; Tidor, B.; Rana, T. M.; Schiffer, C. A.; Gilson, M. K. Design of Mutation-Resistant HIV Protease Inhibitors with the Substrate Envelope Hypothesis. *Chem. Biol. Drug Des.* **2007**, *69*, 298–313.
- (99) Prabu-Jeyabalan, M.; King, N. M.; Nalivaika, E. A.; Heilek-Snyder, G.; Cammack, N.; Schiffer, C. A. Substrate Envelope and Drug Resistance: Crystal Structure of RO1 in Complex with Wild-Type Human Immunodeficiency Virus Type 1 Protease. *Antimicrob. Agents Chemother.* **2006**, *50*, 1518–21.
- (100) King, N. M.; Prabu-Jeyabalan, M.; Nalivaika, E. A.; Wigerinck, P.; de Bethune, M. P.; Schiffer, C. A. Structural and Thermodynamic Basis for the Binding of TMC114, a Next-Generation Human Immunodeficiency Virus Type 1 Protease Inhibitor. *J. Virol.* **2004**, *78*, 12012–21.
- (101) King, N. M.; Prabu-Jeyabalan, M.; Nalivaika, E. A.; Schiffer, C. A. Combating Susceptibility to Drug Resistance: Lessons from HIV-1 Protease. *Chem. Biol.* **2004**, *11*, 1333–8.
- (102) Nalam, M. N.; Ali, A.; Reddy, G. S.; Cao, H.; Anjum, S. G.; Altman, M. D.; Yilmaz, N. K.; Tidor, B.; Rana, T. M.; Schiffer, C. A. Substrate Envelope-Designed Potent HIV-1 Protease Inhibitors To Avoid Drug Resistance. *Chem. Biol.* **2013**, *20*, 1116–24.
- (103) Shen, Y.; Altman, M. D.; Ali, A.; Nalam, M. N.; Cao, H.; Rana, T. M.; Schiffer, C. A.; Tidor, B. Testing the Substrate-Envelope Hypothesis with Designed Pairs of Compounds. *ACS Chem. Biol.* **2013**, *8*, 2433–41.
- (104) Nalam, M. N.; Schiffer, C. A. New Approaches to HIV Protease Inhibitor Drug Design II: Testing the Substrate Envelope Hypothesis To Avoid Drug Resistance and Discover Robust Inhibitors. *Curr. Opin. HIV AIDS* **2008**, *3*, 642–6.
- (105) Chusacutanachai, S.; Thiensathit, P.; Tarnchompoo, B.; Sirawaraporn, W.; Yuthavong, Y. Novel Antifolate Resistant Mutations of *Plasmodium falciparum* Dihydrofolate Reductase Selected in *Escherichia coli*. *Mol. Biochem. Parasitol.* **2002**, *120*, 61–72.
- (106) Japrun, D.; Leartsakulpanich, U.; Chusacutanachai, S.; Yuthavong, Y. Conflicting Requirements of *Plasmodium falciparum* Dihydrofolate Reductase Mutations Conferring Resistance to Pyrimethamine–WR99210 Combination. *Antimicrob. Agents Chemother.* **2007**, *51*, 4356–60.
- (107) Kamchonwongpaisan, S.; Vanichtanankul, J.; Taweechai, S.; Chitnumsub, P.; Yuthavong, Y. The Role of Tryptophan-48 in Catalysis and Binding of Inhibitors of *Plasmodium falciparum* Dihydrofolate Reductase. *Int. J. Parasitol.* **2007**, *37*, 787–93.
- (108) Maitarad, P.; Kamchonwongpaisan, S.; Vanichtanankul, J.; Vilaivan, T.; Yuthavong, Y.; Hannongbua, S. Interactions between Cycloquanil Derivatives and Wild Type and Resistance-Associated Mutant *Plasmodium falciparum* Dihydrofolate Reductases. *J. Comput.-Aided Mol. Des.* **2009**, *23*, 241–52.
- (109) Yuthavong, Y.; Yuvaniyama, J.; Chitnumsub, P.; Vanichtanankul, J.; Chusacutanachai, S.; Tarnchompoo, B.; Vilaivan, T.; Kamchonwongpaisan, S. Malarial (*Plasmodium falciparum*) Dihydrofolate Reductase-Thymidylate Synthase: Structural Basis for Antifolate Resistance and Development of Effective Inhibitors. *Parasitology* **2005**, *130*, 249–59.
- (110) Lin, Y. C.; Perryman, A. L.; Olson, A. J.; Torbett, B. E.; Elder, J. H.; Stout, C. D. Structural Basis for Drug and Substrate Specificity Exhibited by FIV Encoding a Chimeric FIV/HIV Protease. *Acta Crystallogr., Sect. D: Biol. Crystallogr.* **2011**, *67*, 540–8.



- (111) Ekins, S.; Clark, A. M.; Sarker, M. TB Mobile: A Mobile App for Anti-Tuberculosis Molecules with Known Targets. *J. Cheminf.* **2013**, *5*, No. 13.
- (112) Clark, A. M.; Sarker, M.; Ekins, S. New Target Prediction and Visualization Tools Incorporating Open Source Molecular Fingerprints for TB Mobile 2.0. *J. Cheminf.* **2014**, *6*, No. 38.
- (113) *Discovery Studio Modeling Environment*, release 4.0; Accelrys Software: San Diego, CA, 2013.
- (114) Willett, P. Similarity-Based Virtual Screening Using 2D Fingerprints. *Drug Discovery Today* **2006**, *11*, 1046–53.
- (115) Ballell, L.; Bates, R. H.; Young, R. J.; Alvarez-Gomez, D.; Alvarez-Ruiz, E.; Barroso, V.; Blanco, D.; Crespo, B.; Escribano, J.; Gonzalez, R.; Lozano, S.; Huss, S.; Santos-Villarejo, A.; Martin-Plaza, J. J.; Mendoza, A.; Rebollo-Lopez, M. J.; Remuinan-Blanco, M.; Lavandera, J. L.; Perez-Herran, E.; Gamo-Benito, F. J.; Garcia-Bustos, J. F.; Barros, D.; Castro, J. P.; Cammack, N. Fueling Open-Source Drug Discovery: 177 Small-Molecule Leads against Tuberculosis. *ChemMedChem* **2013**, *8*, 313–21.
- (116) Franzblau, S. G.; Witzig, R. S.; McLaughlin, J. C.; Torres, P.; Madico, G.; Hernandez, A.; Degnan, M. T.; Cook, M. B.; Quenzer, V. K.; Ferguson, R. M.; Gilman, R. H. Rapid, Low-Technology MIC Determination with Clinical *Mycobacterium tuberculosis* Isolates by Using the Microplate Alamar Blue Assay. *J. Clin. Microbiol.* **1998**, *36*, 362–6.
- (117) Chessari, G.; Woodhead, A. J. From Fragment to Clinical Candidate—A Historical Perspective. *Drug Discovery Today* **2009**, *14*, 668–75.
- (118) Hajduk, P. J.; Greer, J. A Decade of Fragment-Based Drug Design: Strategic Advances and Lessons Learned. *Nat. Rev. Drug Discovery* **2007**, *6*, 211–9.
- (119) Austin, C.; Pettit, S. N.; Magnolo, S. K.; Sanvoisin, J.; Chen, W.; Wood, S. P.; Freeman, L. D.; Pengelly, R. J.; Hughes, D. E. Fragment Screening Using Capillary Electrophoresis (CEfrag) for Hit Identification of Heat Shock Protein 90 ATPase Inhibitors. *J. Biomol. Screening* **2012**, *17*, 868–76.
- (120) Teotico, D. G.; Babaoglu, K.; Rocklin, G. J.; Ferreira, R. S.; Giannetti, A. M.; Shoichet, B. K. Docking for Fragment Inhibitors of AmpC  $\beta$ -Lactamase. *Proc. Natl. Acad. Sci. U.S.A.* **2009**, *106*, 7455–7460.
- (121) Murray, C. W.; Callaghan, O.; Chessari, G.; Cleasby, A.; Congreve, M.; Frederickson, M.; Hartshorn, M. J.; McMenamin, R.; Patel, S.; Wallis, N. Application of Fragment Screening by X-ray Crystallography to  $\beta$ -Secretase. *J. Med. Chem.* **2007**, *50*, 1116–23.
- (122) Chen, Y.; Shoichet, B. K. Molecular Docking and Ligand Specificity in Fragment-Based Inhibitor Discovery. *Nat. Chem. Biol.* **2009**, *5*, 358–64.
- (123) Shuker, S. B.; Hajduk, P. J.; Meadows, R. P.; Fesik, S. W. Discovering High-Affinity Ligands for Proteins: SAR by NMR. *Science* **1996**, *274*, 1531–4.
- (124) Li, H. J.; Lai, C. T.; Pan, P.; Yu, W.; Liu, N.; Bommineni, G. R.; Garcia-Diaz, M.; Simmerling, C.; Tonge, P. J. A Structural and Energetic Model for the Slow-Onset Inhibition of the *Mycobacterium tuberculosis* Enoyl-ACP Reductase InhA. *ACS Chem. Biol.* **2014**, *9*, 986–93.
- (125) am Ende, C. W.; Knudson, S. E.; Liu, N.; Childs, J.; Sullivan, T. J.; Boyne, M.; Xu, H.; Gagina, Y.; Knudson, D. L.; Johnson, F.; Peloquin, C. A.; Slayden, R. A.; Tonge, P. J. Synthesis and in Vitro Antimycobacterial Activity of B-Ring Modified Diaryl Ether InhA Inhibitors. *Bioorg. Med. Chem. Lett.* **2008**, *18*, 3029–33.
- (126) Bollag, G.; Hirth, P.; Tsai, J.; Zhang, J.; Ibrahim, P. N.; Cho, H.; Spevak, W.; Zhang, C.; Zhang, Y.; Habets, G.; Burton, E. A.; Wong, B.; Tsang, G.; West, B. L.; Powell, B.; Shellooe, R.; Marimuthu, A.; Nguyen, H.; Zhang, K. Y.; Artis, D. R.; Schlessinger, J.; Su, F.; Higgins, B.; Iyer, R.; D'Andrea, K.; Koehler, A.; Stumm, M.; Lin, P. S.; Lee, R. J.; Grippo, J.; Puzanov, I.; Kim, K. B.; Ribas, A.; McArthur, G. A.; Sosman, J. A.; Chapman, P. B.; Flaherty, K. T.; Xu, X.; Nathanson, K. L.; Nolop, K. Clinical Efficacy of a RAF Inhibitor Needs Broad Target Blockade in BRAF-Mutant Melanoma. *Nature* **2010**, *467*, 596–9.
- (127) de Kloe, G. E.; Bailey, D.; Leurs, R.; de Esch, I. J. Transforming Fragments into Candidates: Small Becomes Big in Medicinal Chemistry. *Drug Discovery Today* **2009**, *14*, 630–46.
- (128) Congreve, M.; Chessari, G.; Tisi, D.; Woodhead, A. J. Recent Developments in Fragment-Based Drug Discovery. *J. Med. Chem.* **2008**, *51*, 3661–80.
- (129) Teotico, D. G.; Babaoglu, K.; Rocklin, G. J.; Ferreira, R. S.; Giannetti, A. M.; Shoichet, B. K. Docking for Fragment Inhibitors of AmpC  $\beta$ -Lactamase. *Proc. Natl. Acad. Sci. U.S.A.* **2009**, *106*, 7455–60.
- (130) Krasinski, A.; Radic, Z.; Manetsch, R.; Raushel, J.; Taylor, P.; Sharpless, K. B.; Kolb, H. C. In Situ Selection of Lead Compounds by Click Chemistry: Target-Guided Optimization of Acetylcholinesterase Inhibitors. *J. Am. Chem. Soc.* **2005**, *127*, 6686–92.
- (131) Mamidyala, S. K.; Finn, M. G. In Situ Click Chemistry: Probing the Binding Landscapes of Biological Molecules. *Chem. Soc. Rev.* **2010**, *39*, 1252–61.
- (132) Manetsch, R.; Krasinski, A.; Radic, Z.; Raushel, J.; Taylor, P.; Sharpless, K. B.; Kolb, H. C. In Situ Click Chemistry: Enzyme Inhibitors Made to Their Own Specifications. *J. Am. Chem. Soc.* **2004**, *126*, 12809–18.
- (133) Sharpless, K. B.; Manetsch, R. In Situ Click Chemistry: A Powerful Means for Lead Discovery. *Expert Opin. Drug Discovery* **2006**, *1*, 525–38.